MAGNETIC RECONNECTION IN APPLICATION TO RELATIVISTIC JETS OF ACTIVE GALAXIES

KRZYSZTOF NALEWAJKO

NICOLAUS COPERNICUS ASTRONOMICAL CENTER
POLISH ACADEMY OF SCIENCES

NATIONAL SCIENCE CENTRE
POLAND

Unified Model of Active Galaxies

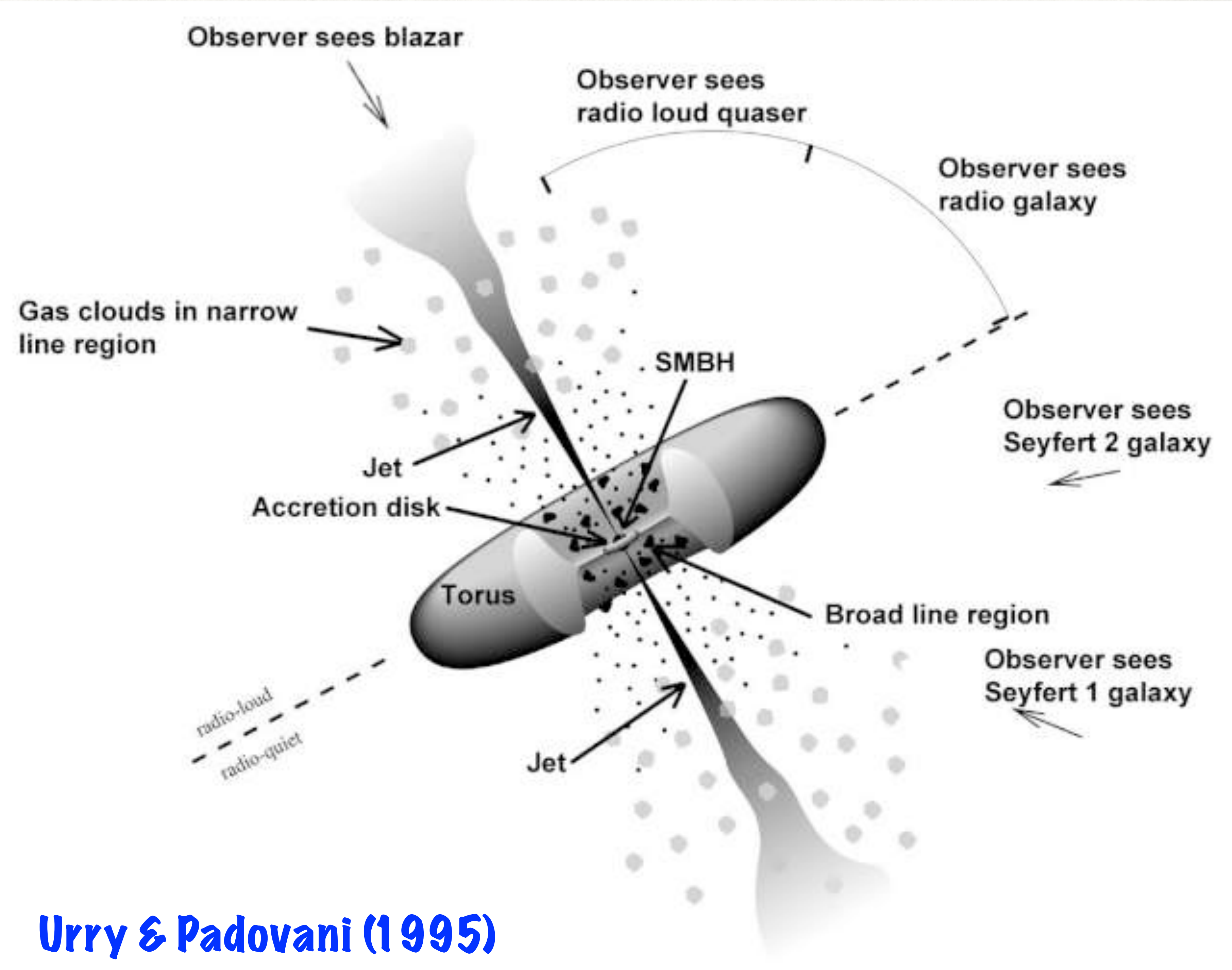

Urry & Padovani (1995)

Spectral Energy Distributions of Blazars

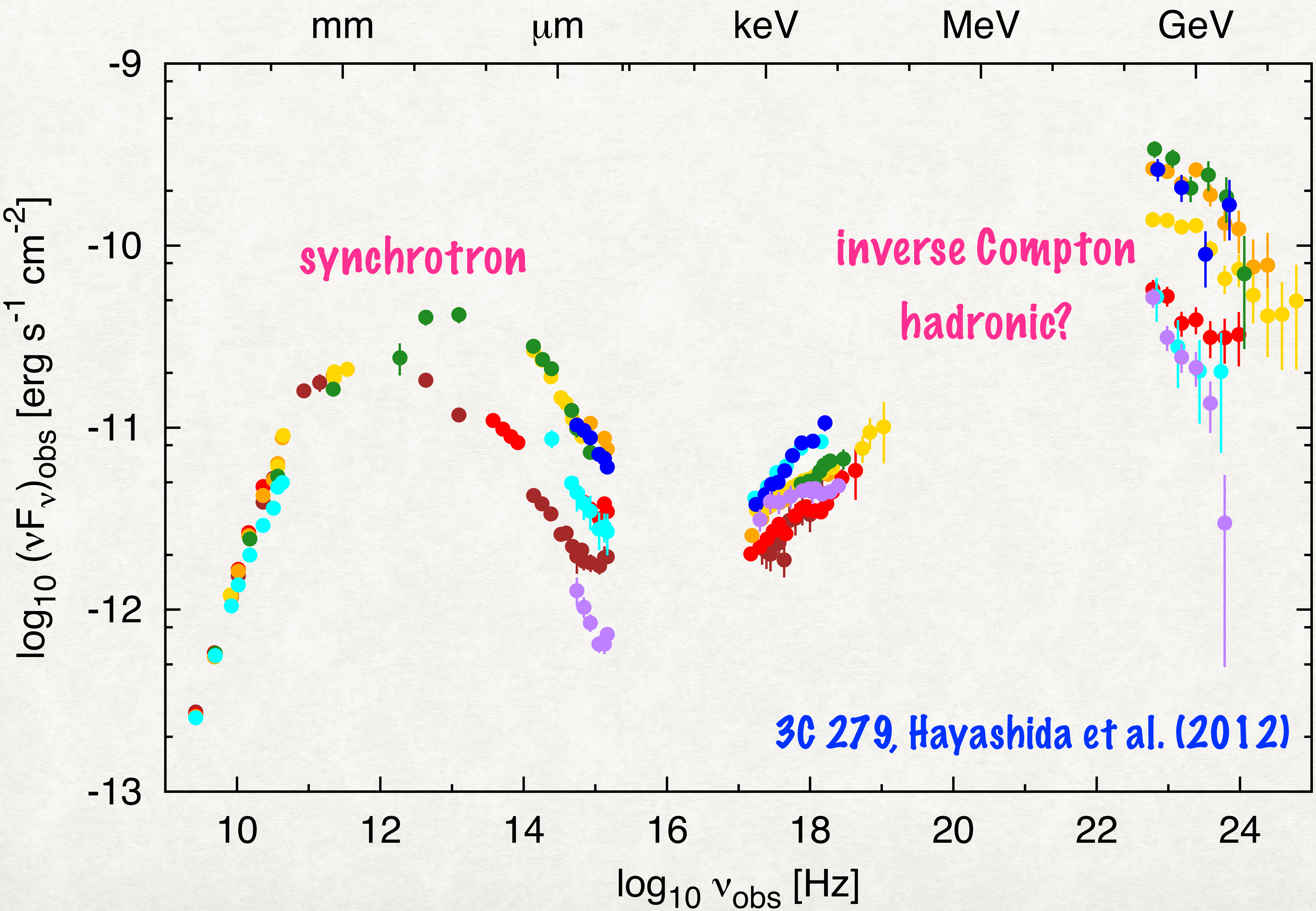

Gamma-ray Variability of Blazars

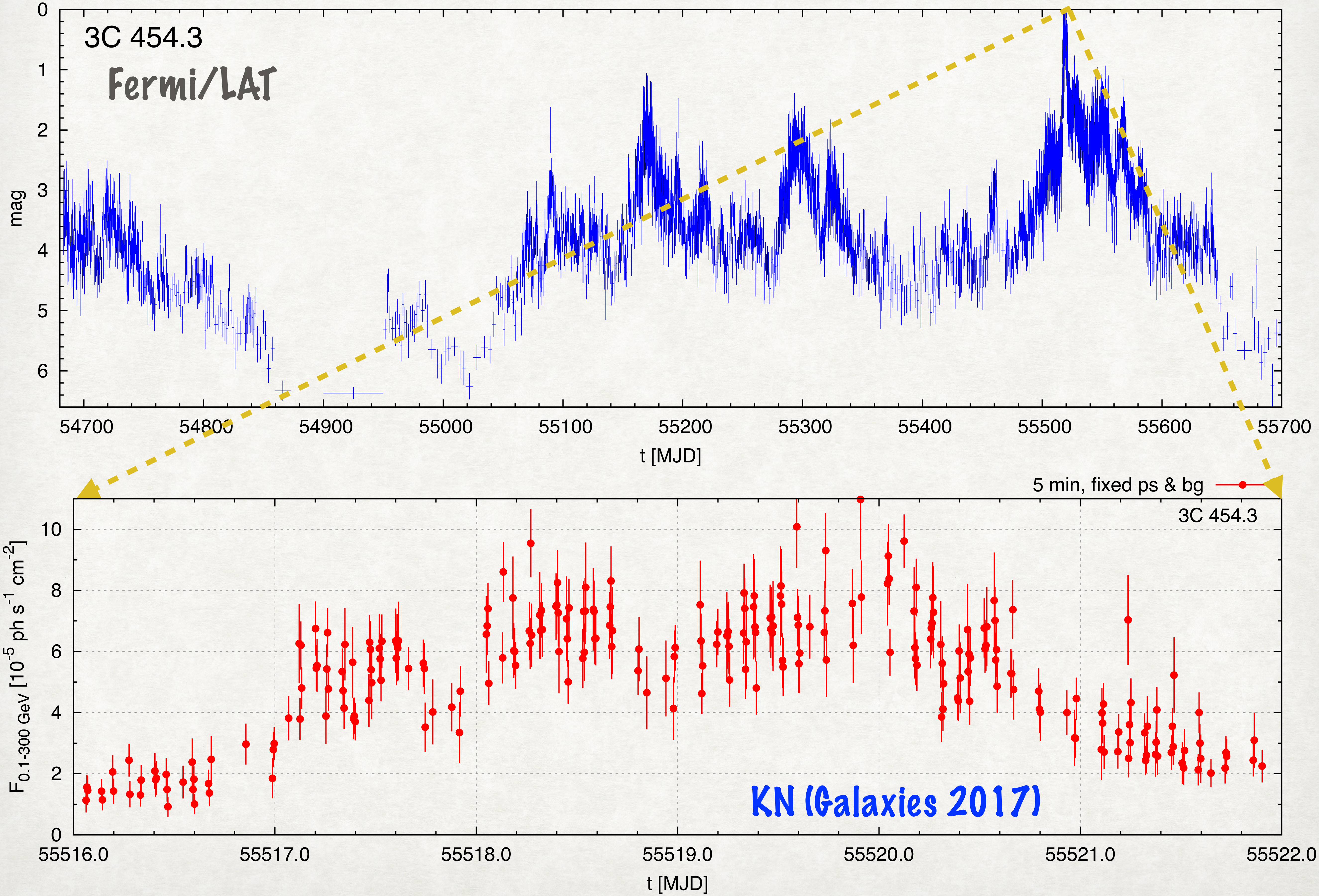

GAMMA-RAY VARIABILITY OF BLAZARS AND MISALIGNED AGNS

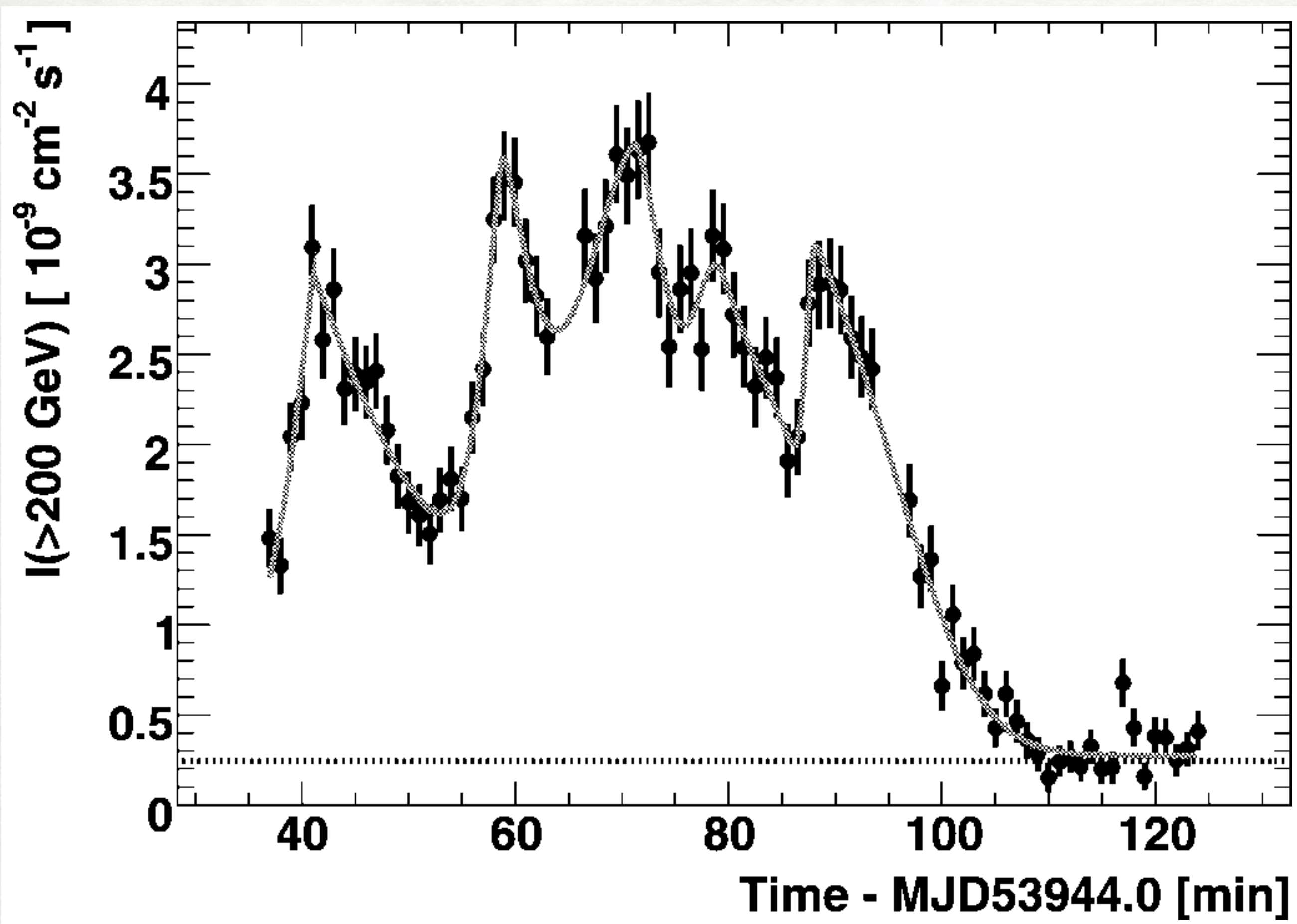

PKS 2155-304
H.E.S.S. Collaboration (2007)

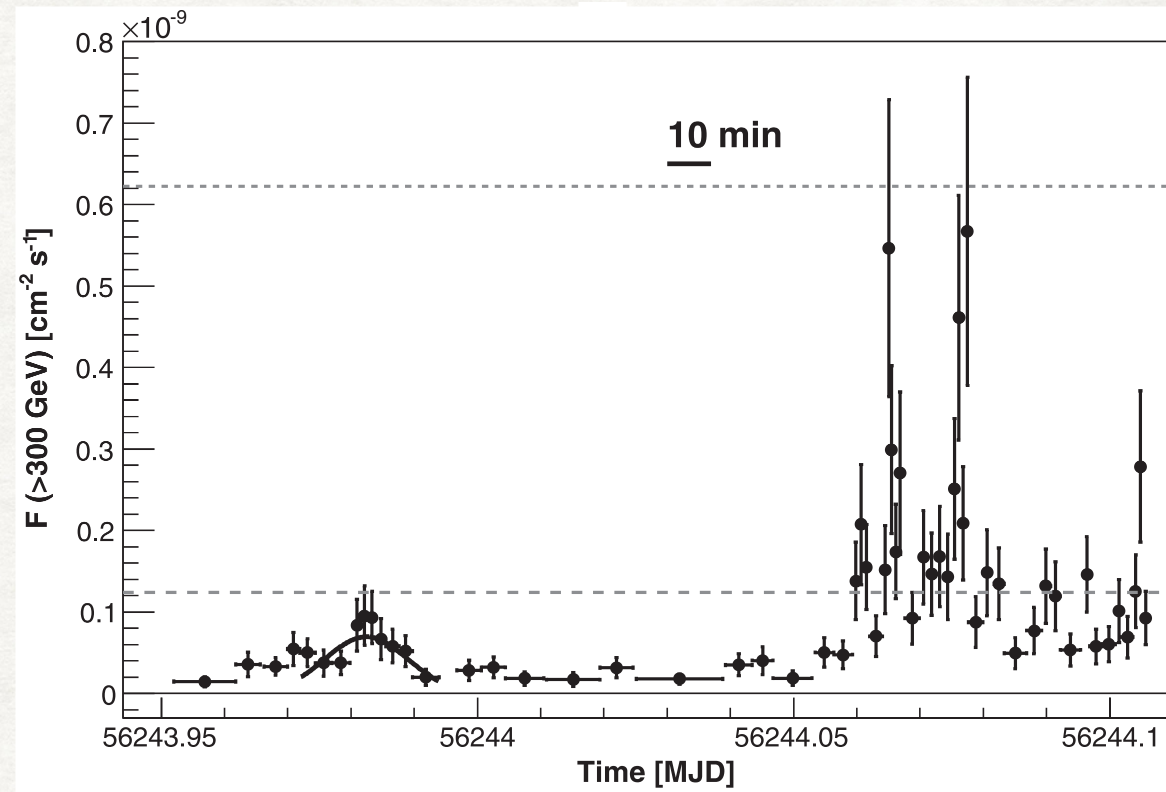

Fig. 4. Light curve of IC 310 observed with the MAGIC telescopes on the night of 12/13 November 2012, above 300 GeV. As a flux reference, the two gray lines indicate levels of 1 and 5 times the flux level of the Crab Nebula, respectively. The precursor flare (MJD 56243.972-56243.994) has been fitted with a Gaussian distribution. Vertical error bars show 1 SD statistical uncertainty. Horizontal error bars show the bin widths.

IC 310
MAGIC Collaboration (2014)

PKS 1222+216

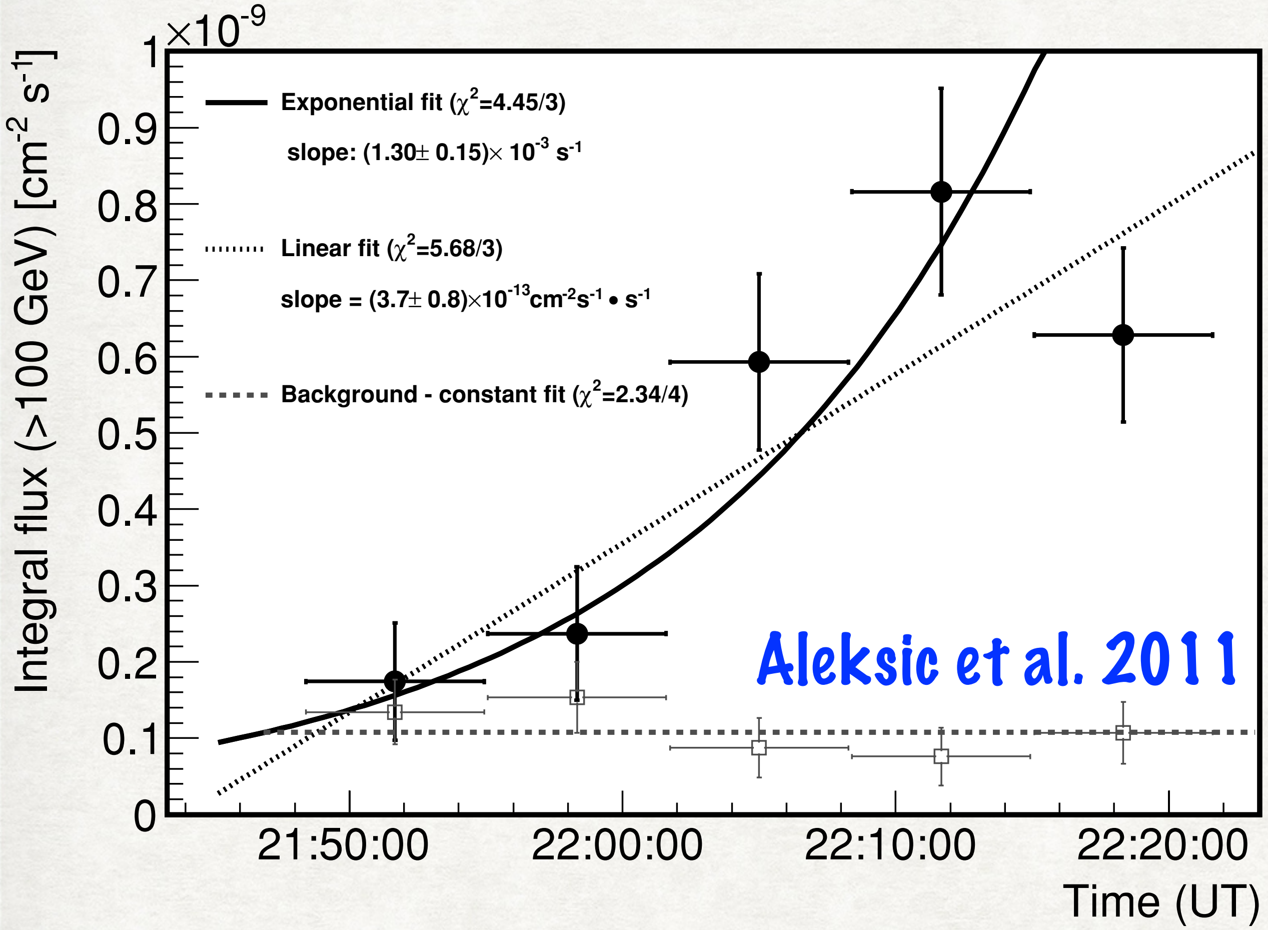

MAGIC (Cerenkov Telescope)

70 - 400 GeV

t_{var} = 10 min

- quasar
- r > 0.5 pc
- R ≲ 8 x 10^{-5} pc (D / 20)
- compactness problem

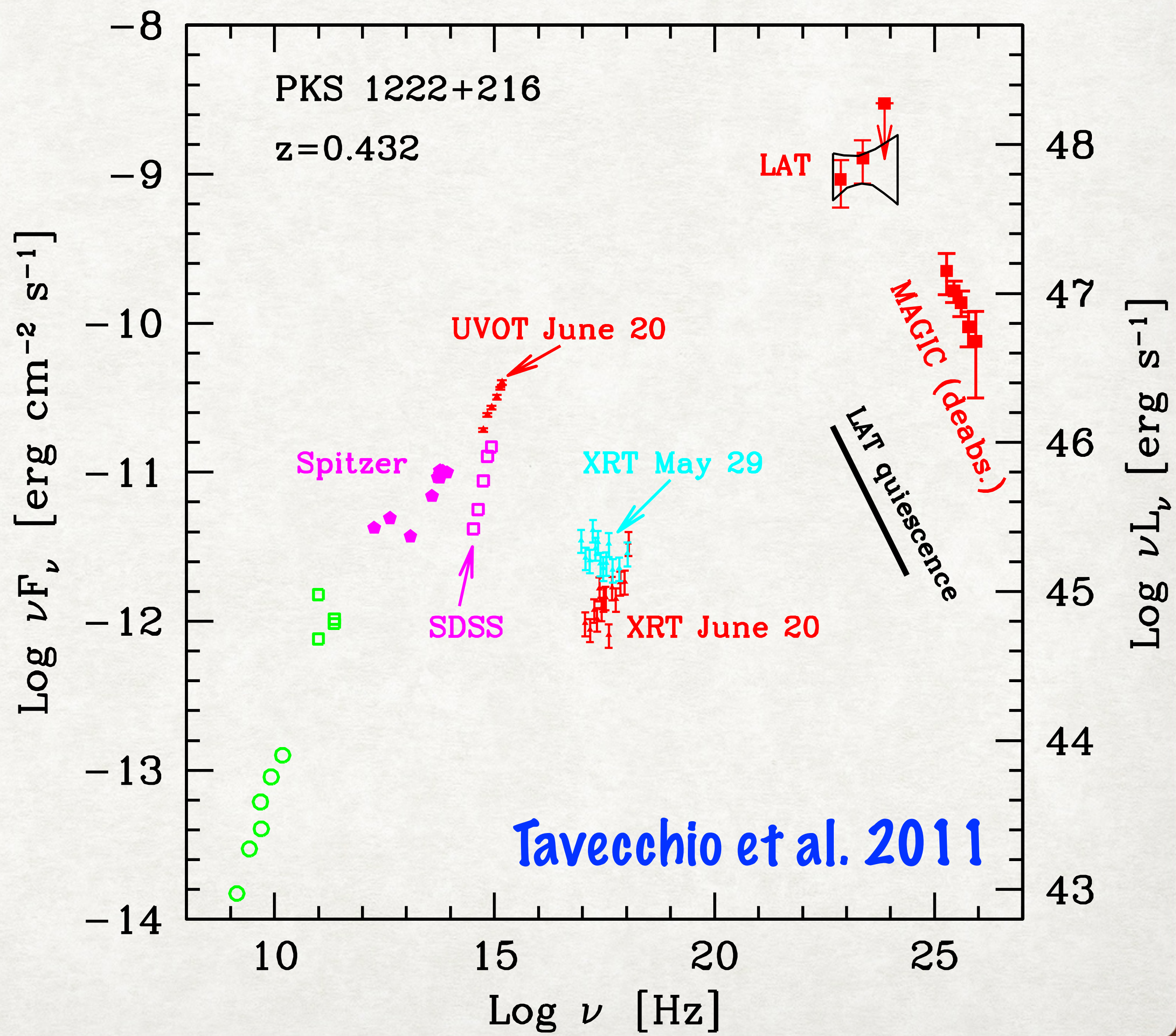

2015 FLARE OF 3C 279

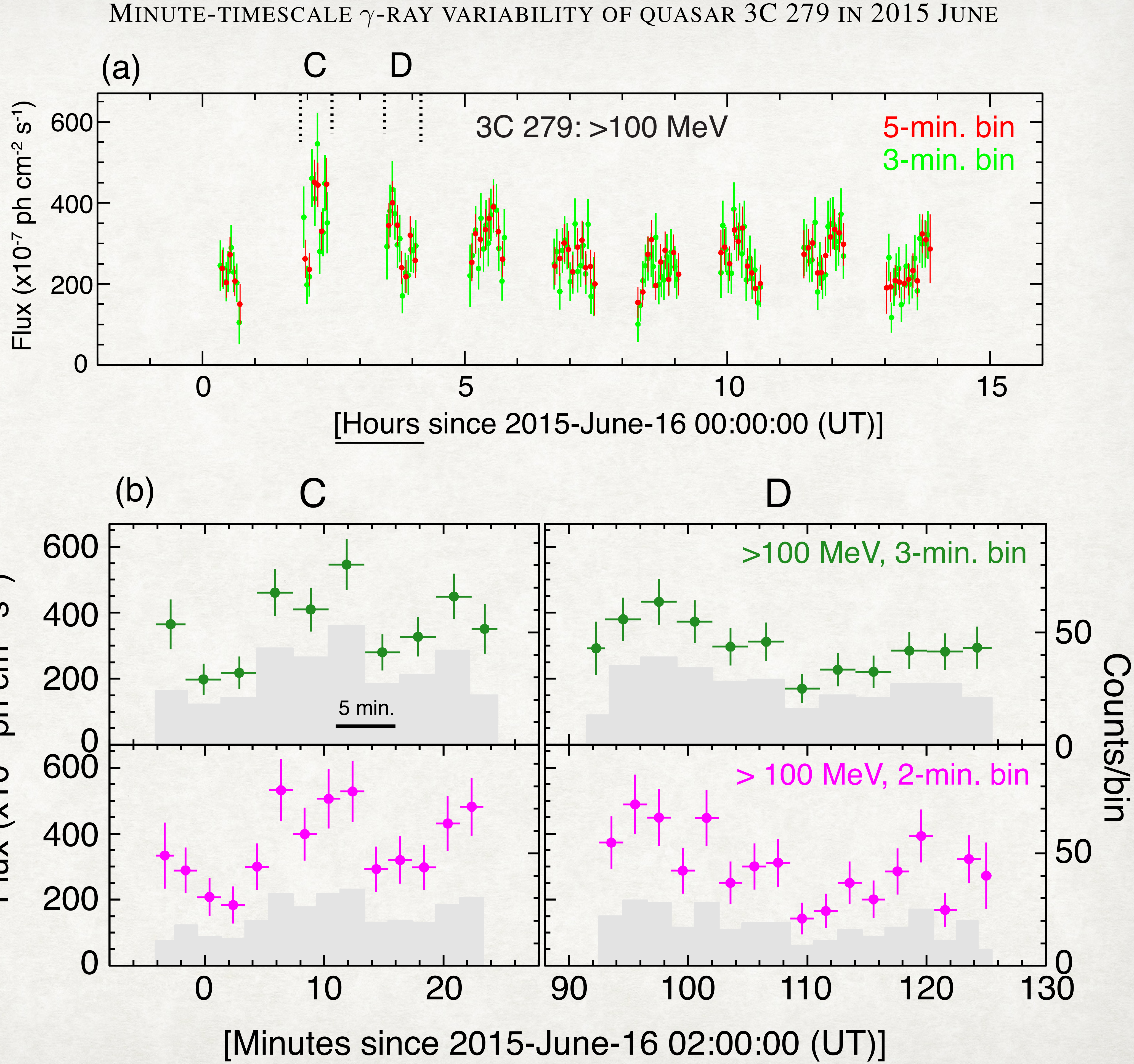

Fermi-LAT Collaboration (Ackermann et al.) (2016)

2018 FLARE OF 3C 279

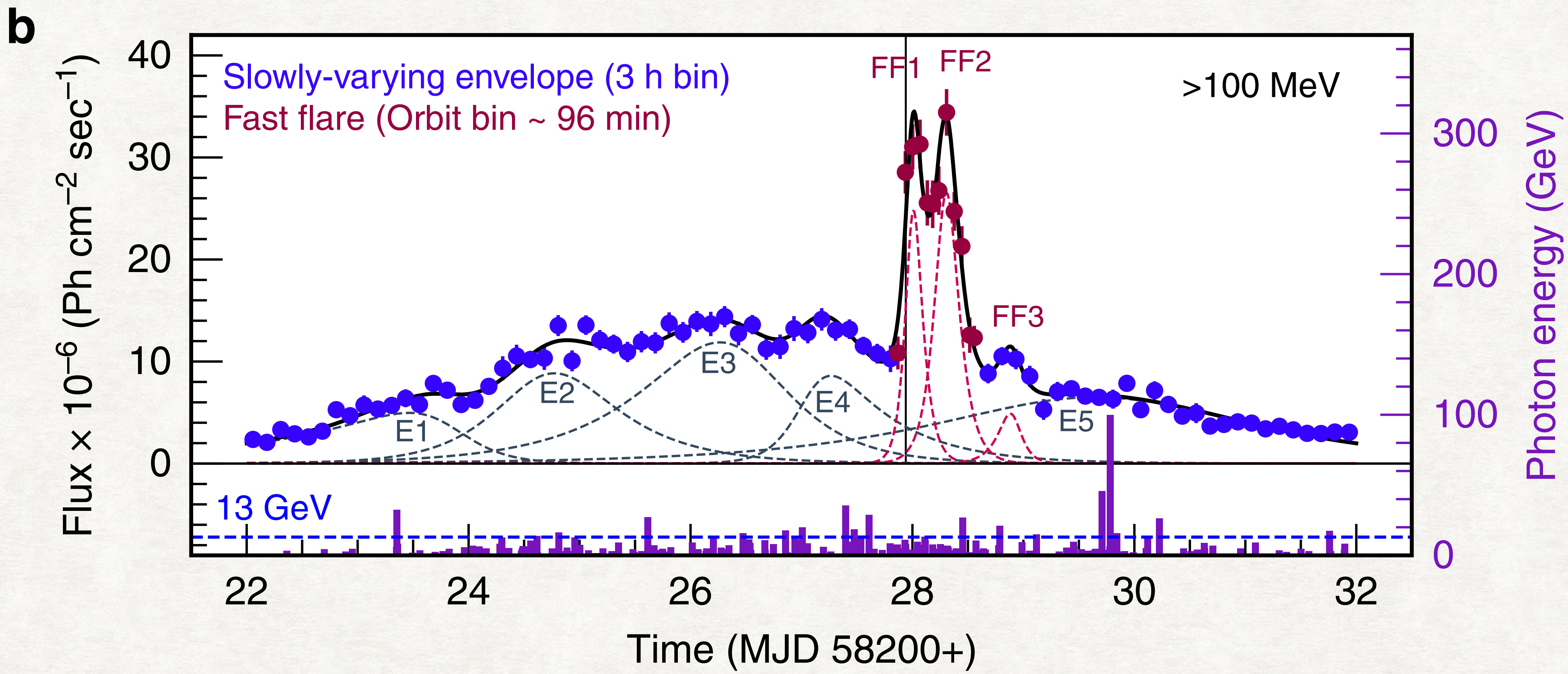

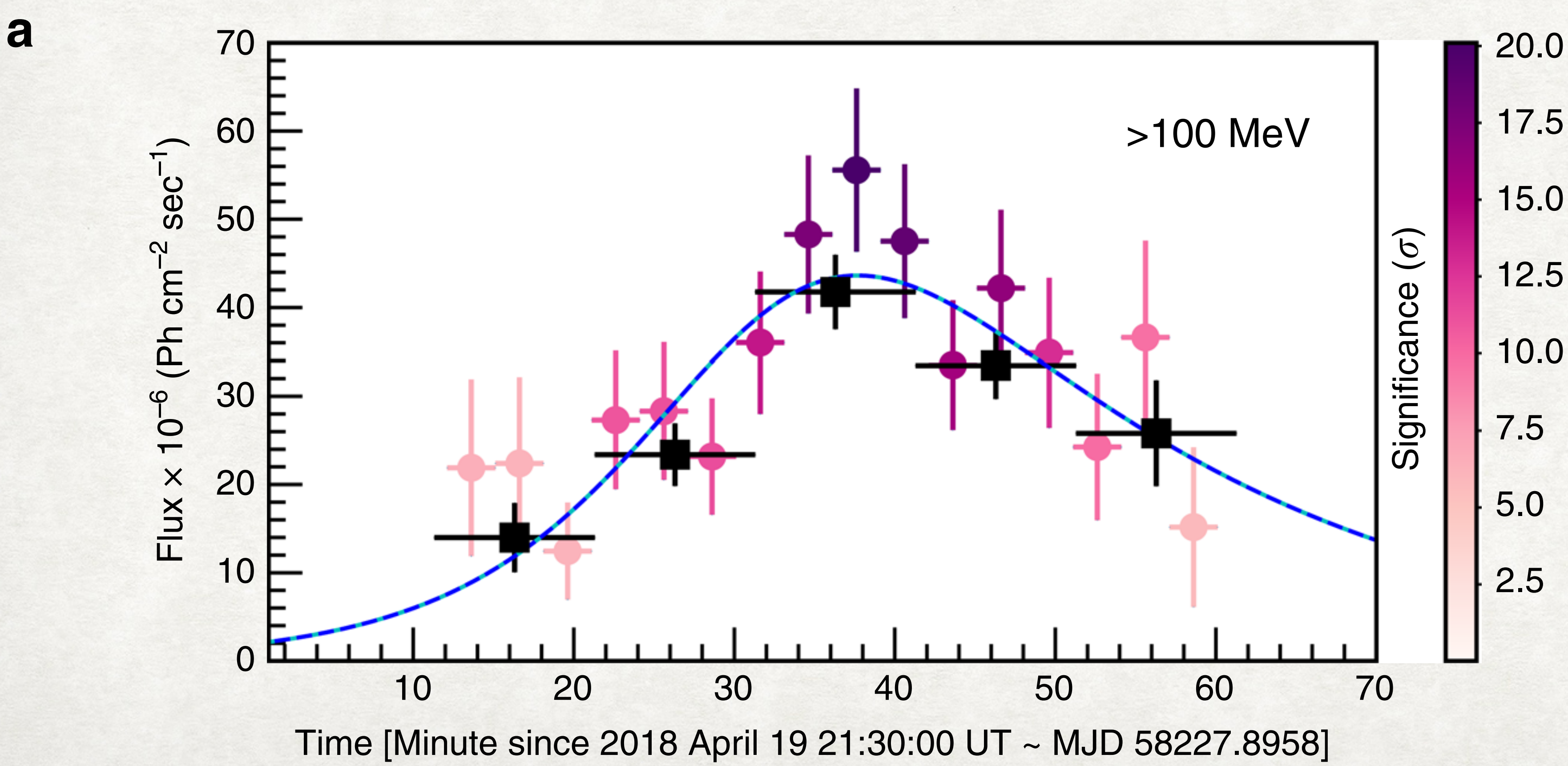

Shukla & Mannheim (Nature Comm. 2020)

Comparing suborbital variations

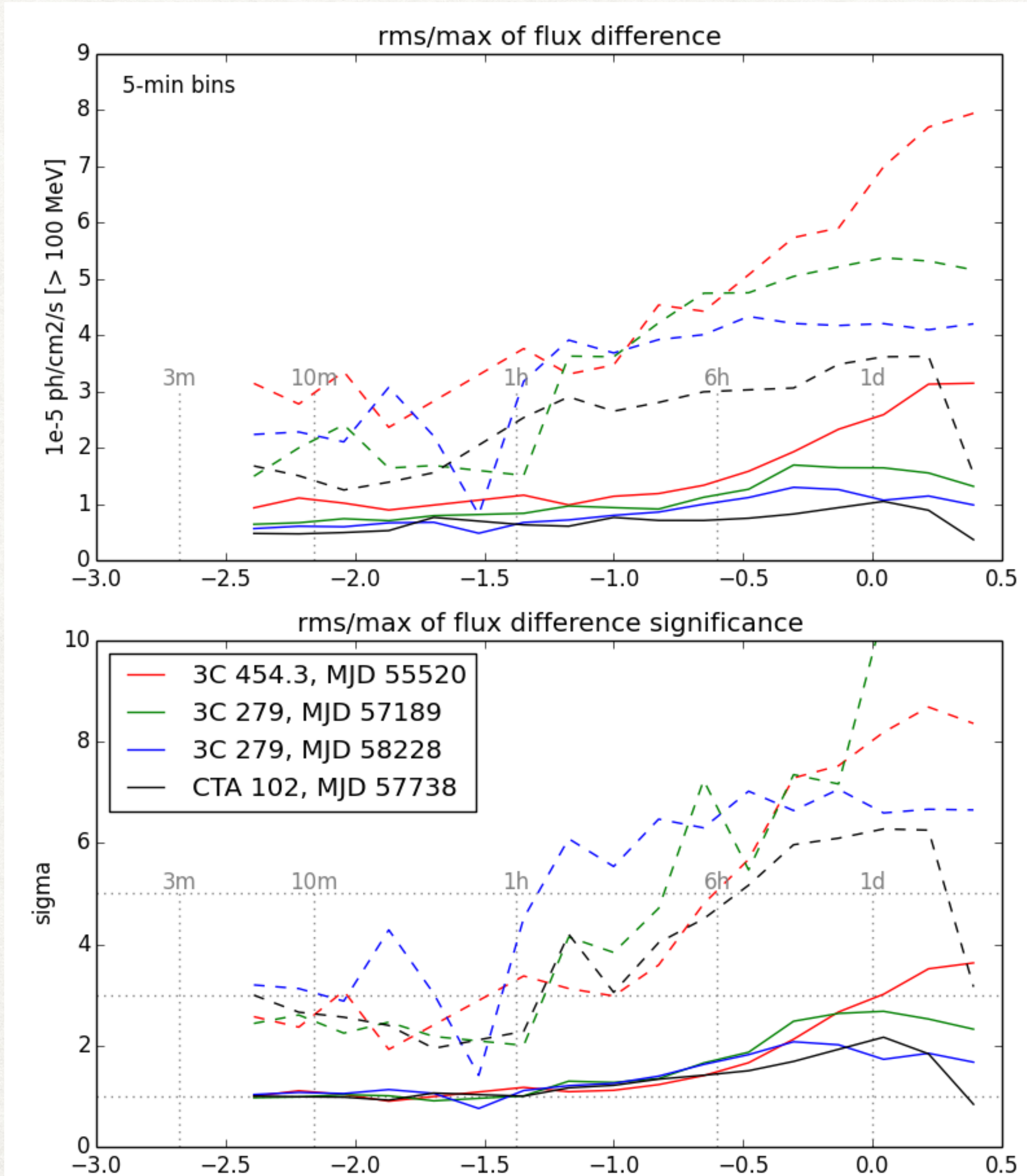

log10 (time scale [d])

see also

KN (Galaxies 2017)

Meyer, Blandford & Scargle (2019)

Rapid GeV Variability in 3C 279

- emitting region size 10^{-4} pc
  dissipation region may be larger by factor 10-100
  distance scale as short as 100 M_{bh}
  gamma-ray opacity (15 GeV)

- **Γ** > 25 from intrinsic opacity, **Γ** > 35 for sub-Eddington jet

- ERC scenario: **Γ** > 50 from SSC constraint
  Γ > 120 from equipartition

- synchrotron scenario: kG B-field, **γ** ~ 10^6
  cf. the Crab flares

- hadronic models: viable at very short distances

Fermi-LAT Collaboration
(Ackermann et al. 2016)

input from M. Hayashida, G. Madejski,
M. Sikora, R. Blandford

MAGNETIZATION OF JETS

- relativistic hot magnetization $\boldsymbol{\sigma} = B^2 / 4\pi w$, where $w = \boldsymbol{\rho} c^2 + e + p$ is the relativistic enthalpy density
- traditional picture: initial $\boldsymbol{\sigma}_{base} \sim 20$ (jet base) converts to $\boldsymbol{\Gamma}_{pc}$ (parsec-scale), leaving $\boldsymbol{\sigma}_{pc} \lesssim 1$
- whether shocks or reconnection, emitting regions close to equipartition, can be very different from the background (Sironi, Petropoulou & Giannios 2015)

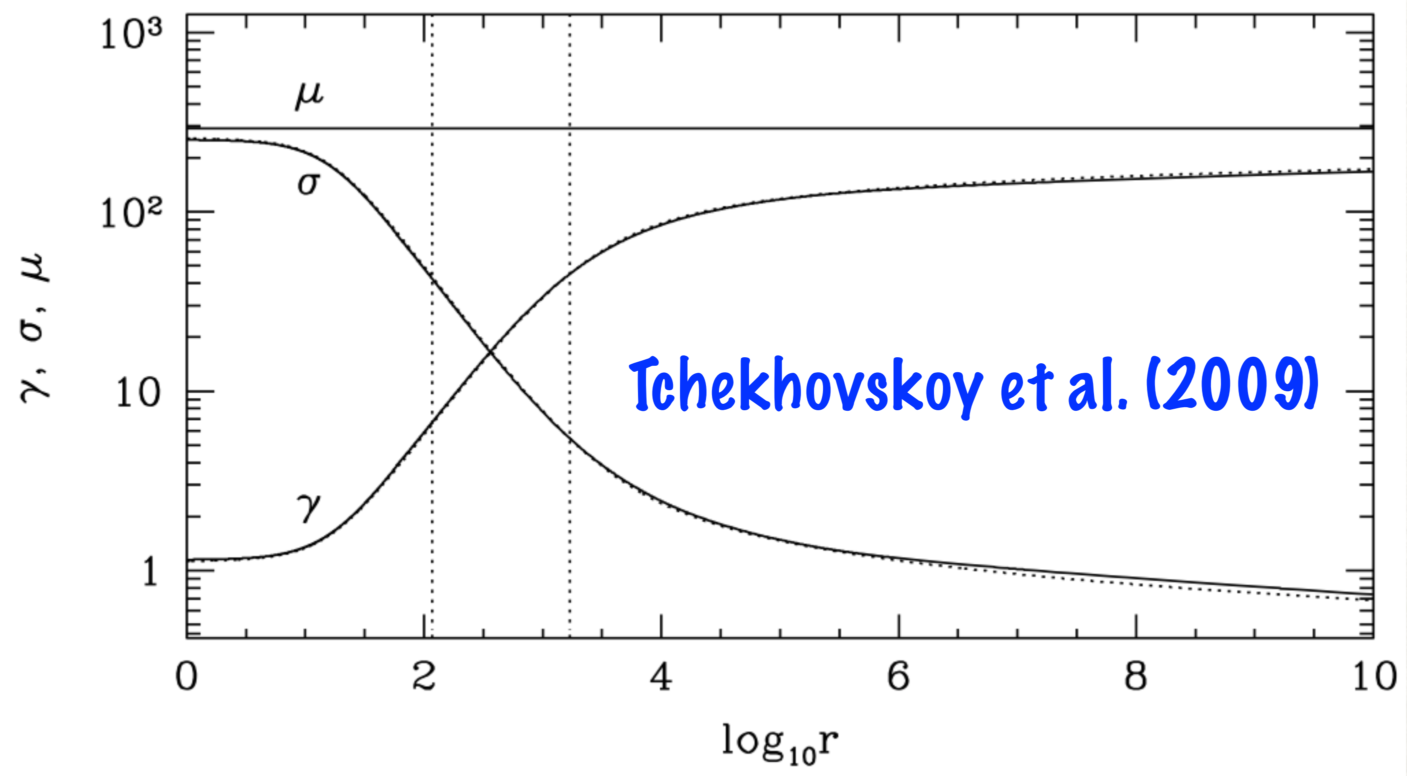

MAGNETIZATION OF JETS

- alternative picture:
  highly inhomogeneous jets due to filamentary loading with protons;
  mean initial magnetization $\langle \boldsymbol{\sigma}_{base} \rangle \sim 20$;
  maximum pc-scale magnetization $\boldsymbol{\sigma}_{pc,max} \sim 10^3$
  required for electron $\gamma_{max} \sim 10^6$ in TeV blazars
  (KN, Galaxies, 2016)

- turbulent magnetic fields enable impulsive particle acceleration despite radiative cooling
  (Zhdankin, Uzdensky, Werner & Begelman 2020)

- turbulent particle energies determined by electron (pair) magnetization:
  $\boldsymbol{\sigma}_{0e} \sim 10^2$ for the FSRQs,
  $\boldsymbol{\sigma}_{0e} \sim 10^3$-$10^6$ for the BL Lacs
  (Sobacchi & Lyubarsky 2020)

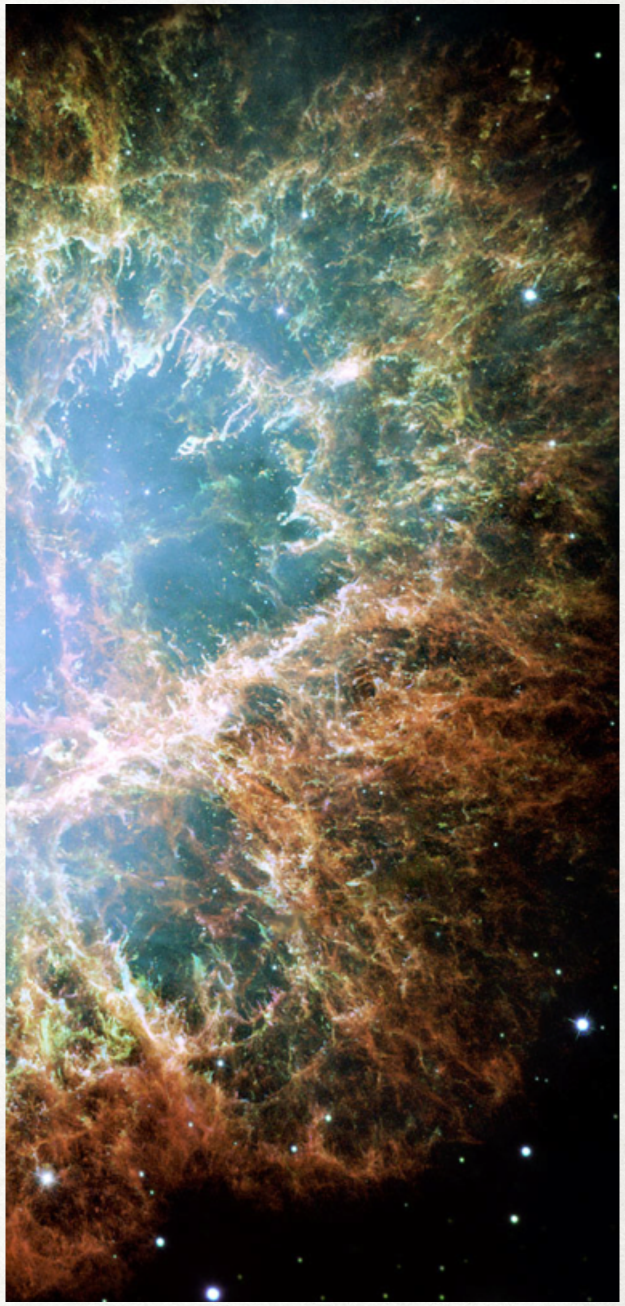

Magnetic Reconnection

magnetic diffusion region (X-point)

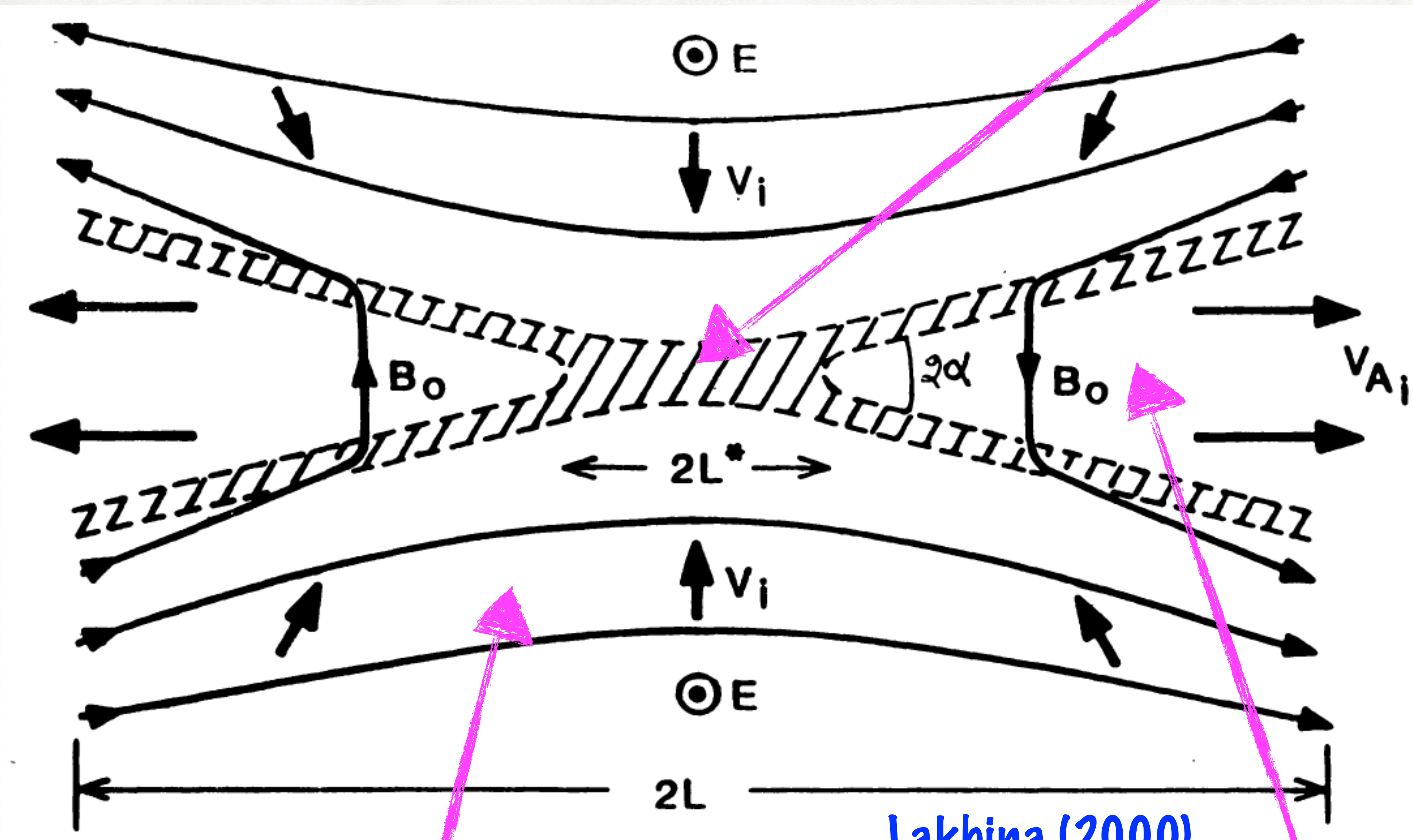

Lakhina (2000)

$E \sim (v_{in}/c)\, B_0$

$v_{in} \sim 0.1\, v_A$

$v_{out} \sim v_A$

reconnecting magnetic field (background, upstream)

reconnection outflow (downstream)

RECONNECTION MODELS

Sweet-Parker

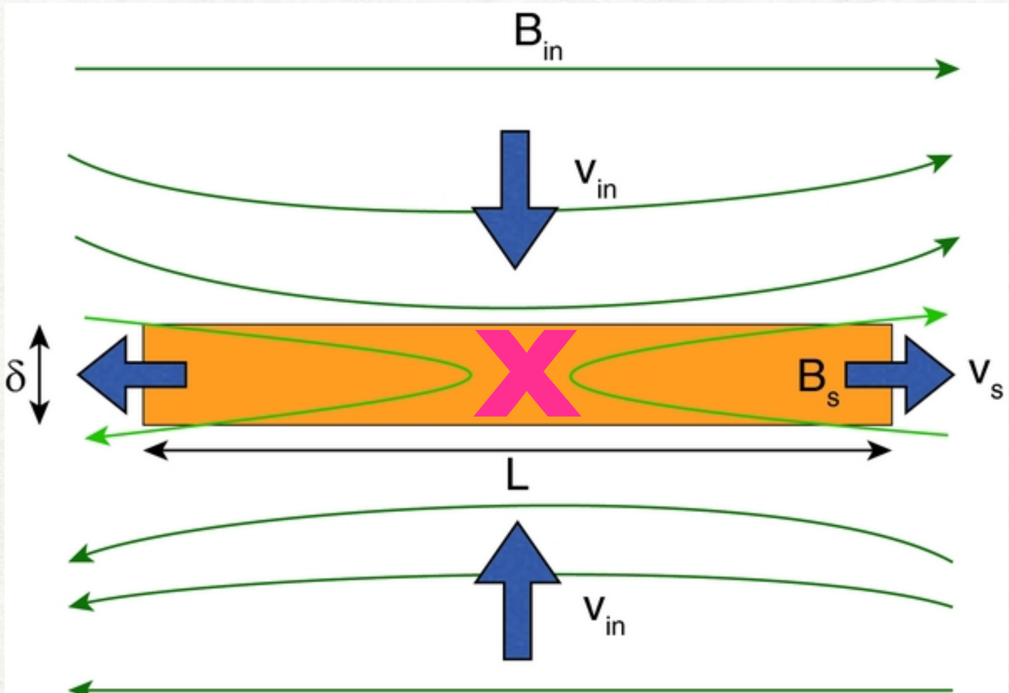

Takamoto (2013)

Petschek

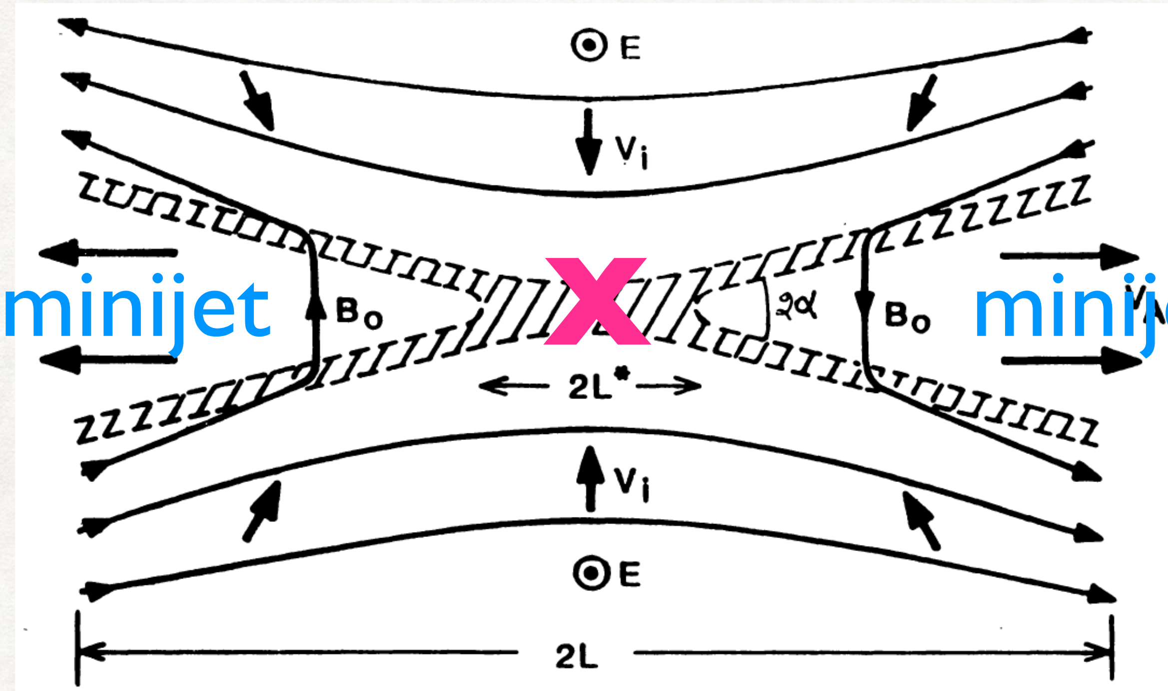

Lakhina (2000)

plasmoid-dominated

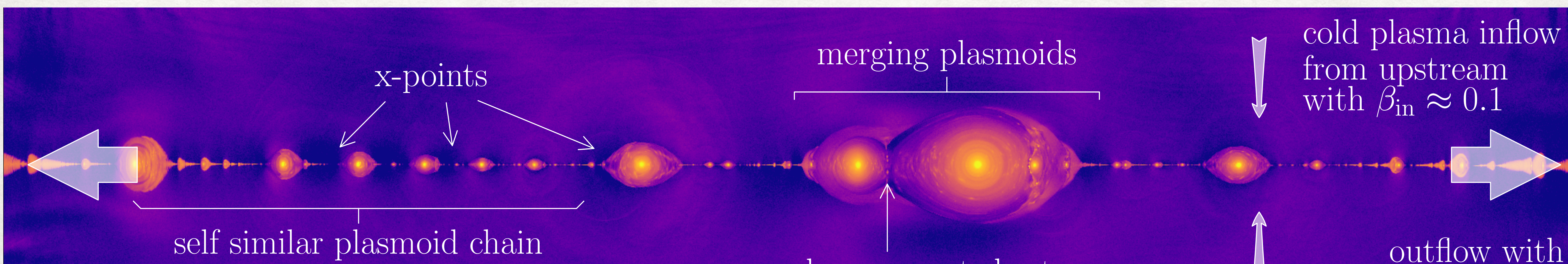

Hakobyan, Philippov & Spitkovsky (2018)

MINIJETS MODEL

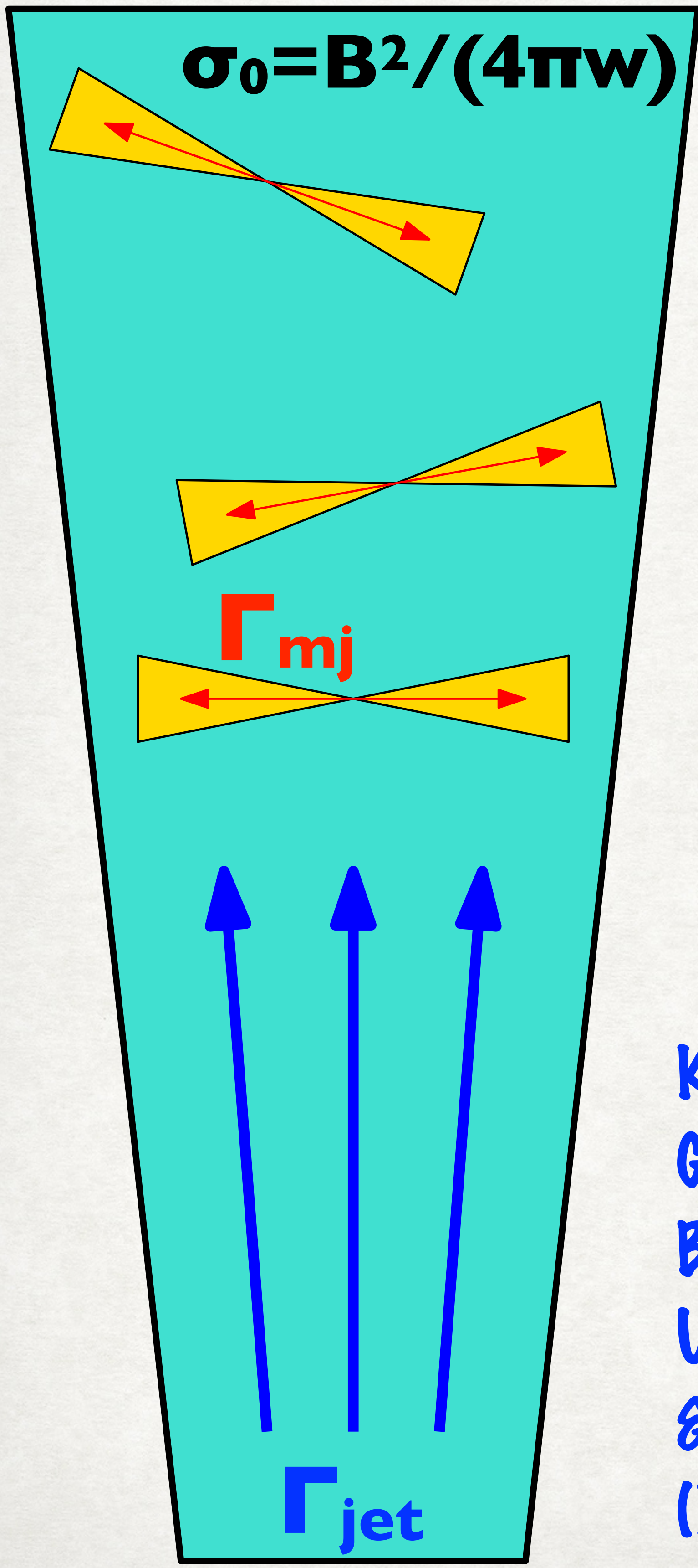

- reconnection produces localized relativistic outflows (minijets) with Γ_{mj} within a larger relativistic jet
- explains additional relativistic Lorentz boost ($\Gamma_{fl} \sim \Gamma_{jet}\Gamma_{mj}$) and local dissipation
- based on relativistic Petschek reconnection model (Lyubarsky 2005)
- depends on the scaling of minijet Lorentz factor with jet magnetization $\Gamma_{mj} \propto \sigma_0^{1/2}$ in relativistic regime (Giannios, Uzdensky & Begelman 2009)

KN, Giannios, Begelman, Uzdensky & Sikora (MNRAS 2011)

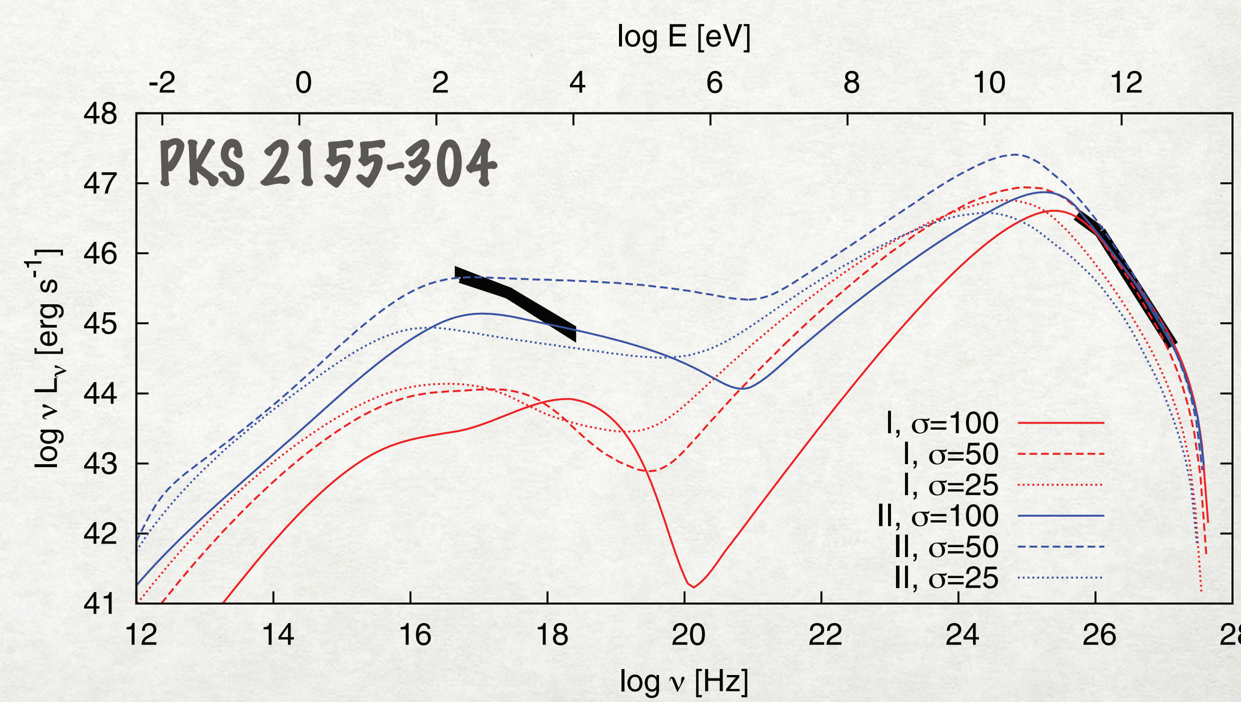

Kinetic Beaming

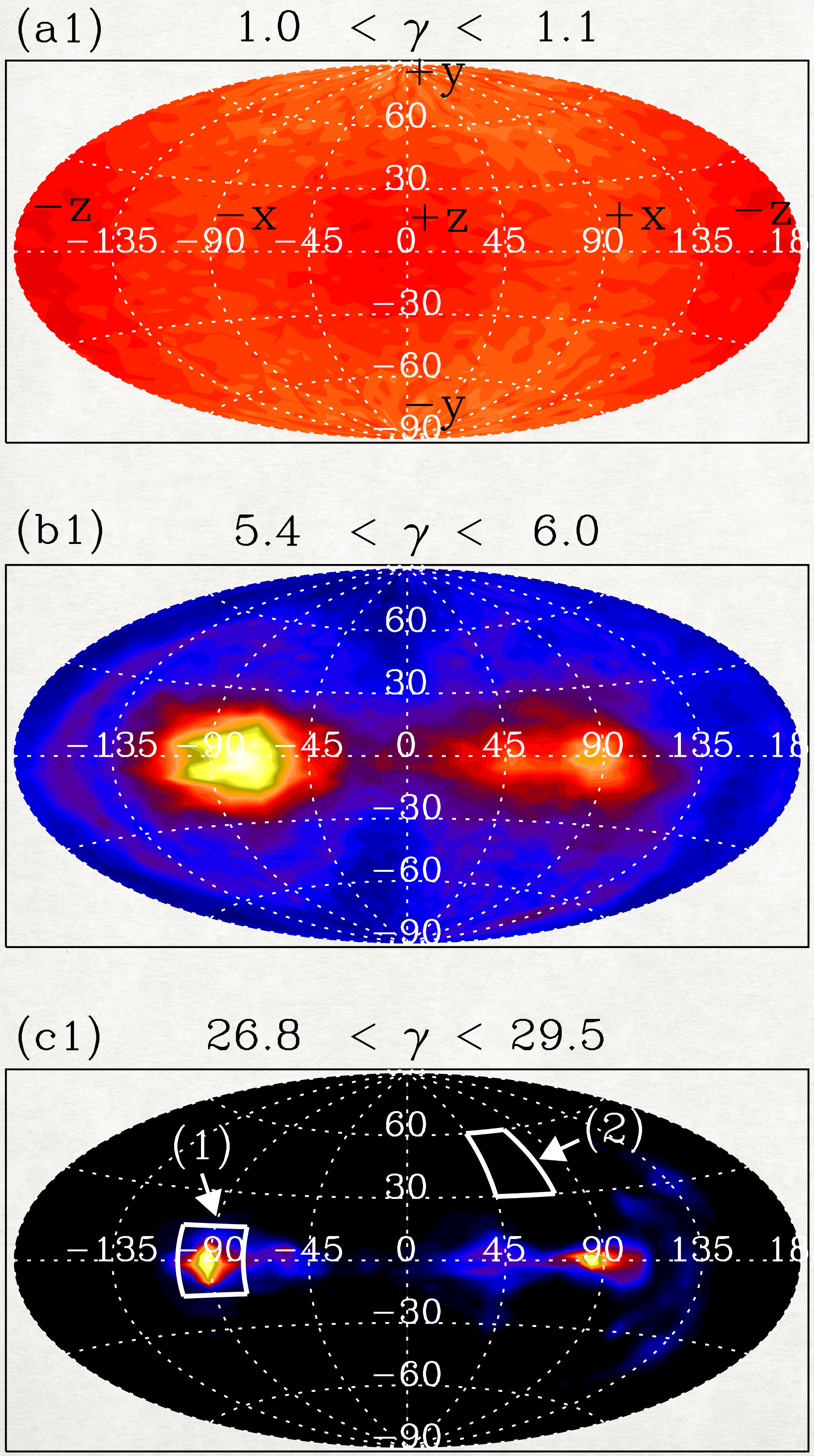

- Anisotropy increasing with particle/photon energy. Rapid variations due to sweeping beams.
- Accelerated particles aligned with magnetic field lines, reduced synchrotron losses.

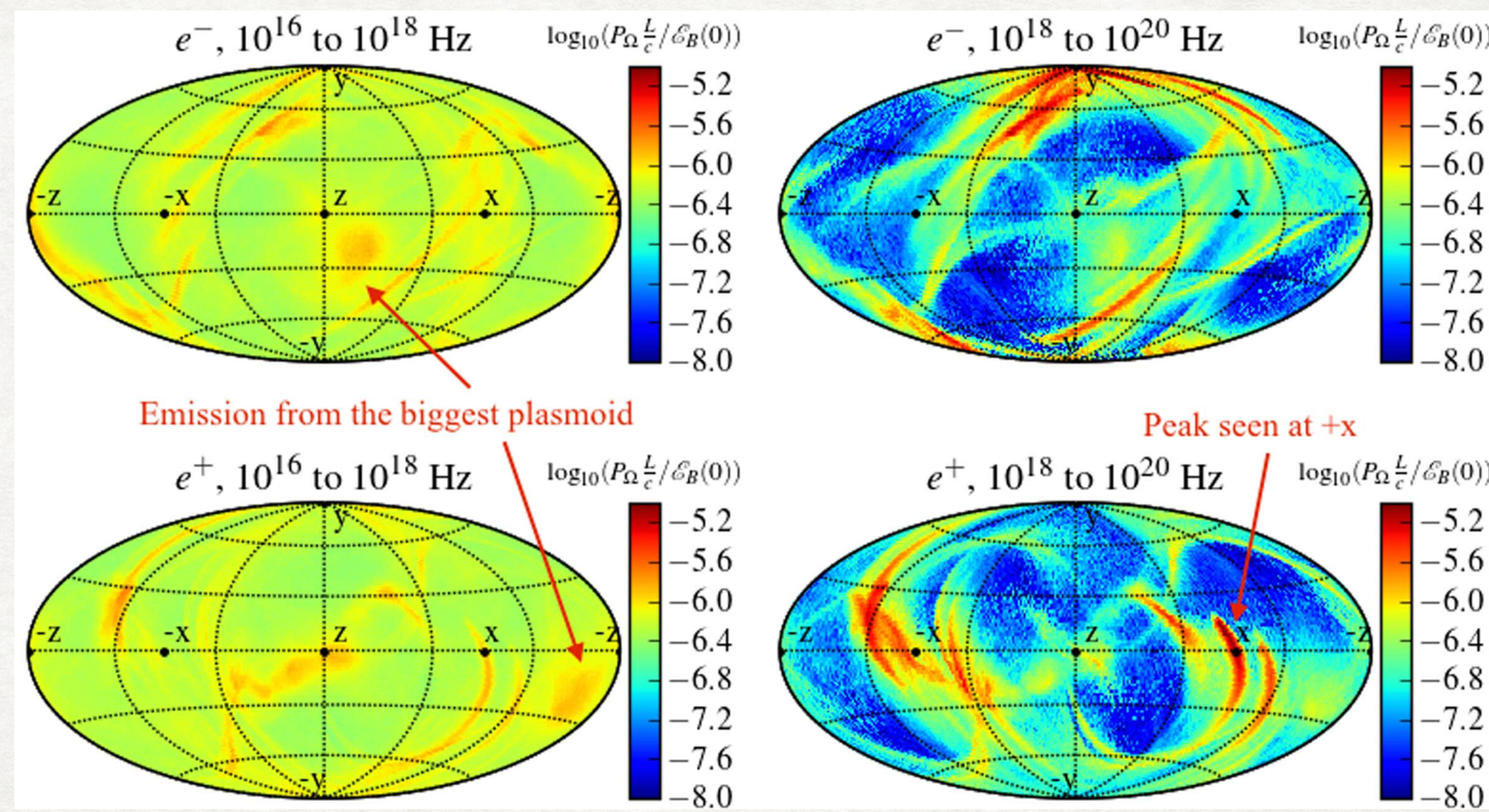

Yuan et al. (2016)

Cerutti et al. (2012)

Hard Particle Spectra in Relativistic Reconnection

- reconnection produces power-law distributions that are hardening with increasing sigma
  $\mathrm{d}N/\mathrm{d}\gamma \propto \gamma^{-p}$ with $p \to 1$ for $\sigma \gg 1$
  (Sironi & Spitkovsky 2014, Guo et al. 2014, Werner et al. 2016)

- high-energy cut-off is exponential with $\gamma_{\max} \sim \mathcal{O}(\sigma)$

- $p \to 2$ in very large plasmoids in 2D
  (Petropoulou & Sironi 2018)

- 3D relativistic reconnection produces hard particle spectra
  $f(\gamma) \propto \gamma^{-p}$ with $p \sim 1.5$
  (Zhang, Sironi & Giannios 2021)

Zhang, Sironi & Giannios (2021)

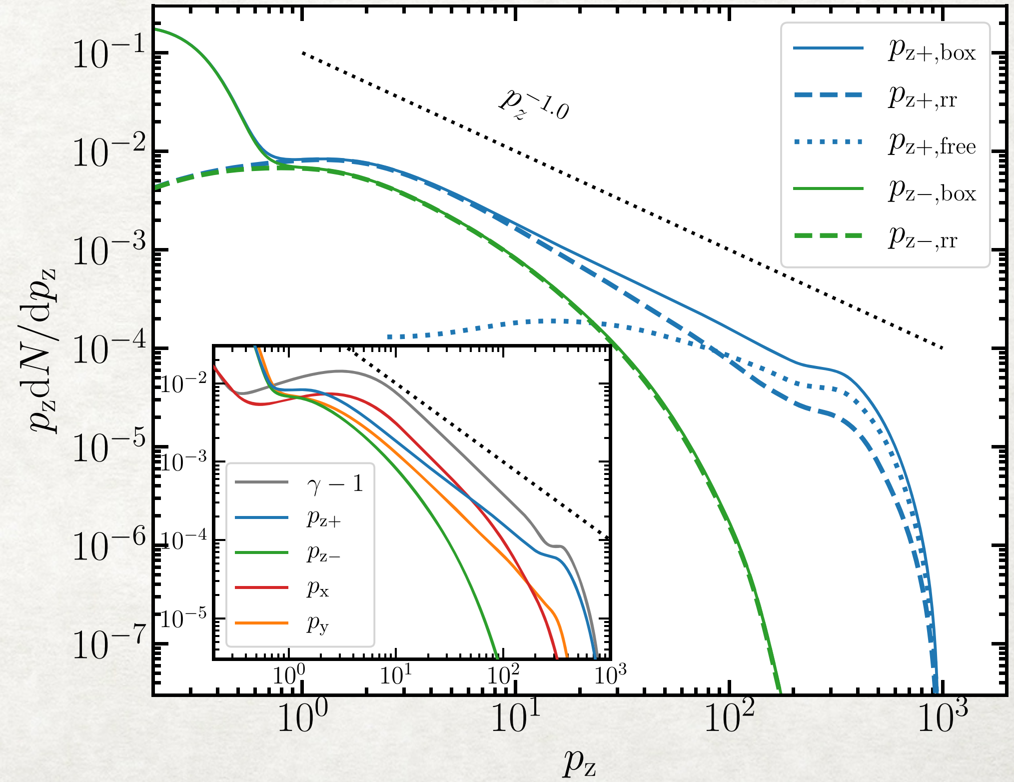

Particle acceleration sites

- **magnetic diffusion regions (X-points):**
  non-ideal E-fields **(Zenitani & Hoshino 2001)**
  most energetic particles pass through them **(Sironi & Spitkovsky 2014)**
  short interaction times **(Guo et al. 2019)**

- **reconnection outflows (minijets):**
  Speiser orbits
  exceeding radiation reaction **(Kirk 2004)**
  low particle density

- **plasmoids:**
  converging "magnetic mirror" **(Drake et al. 2006)**
  particle traps, high particle density
  limited by radiation reaction

- **plasmoid mergers:**
  secondary reconnection layers
  production of rapid and luminous flares **(KN et al. 2015, Ortuño-Macías & KN 2020)**

KN et al. (2015)

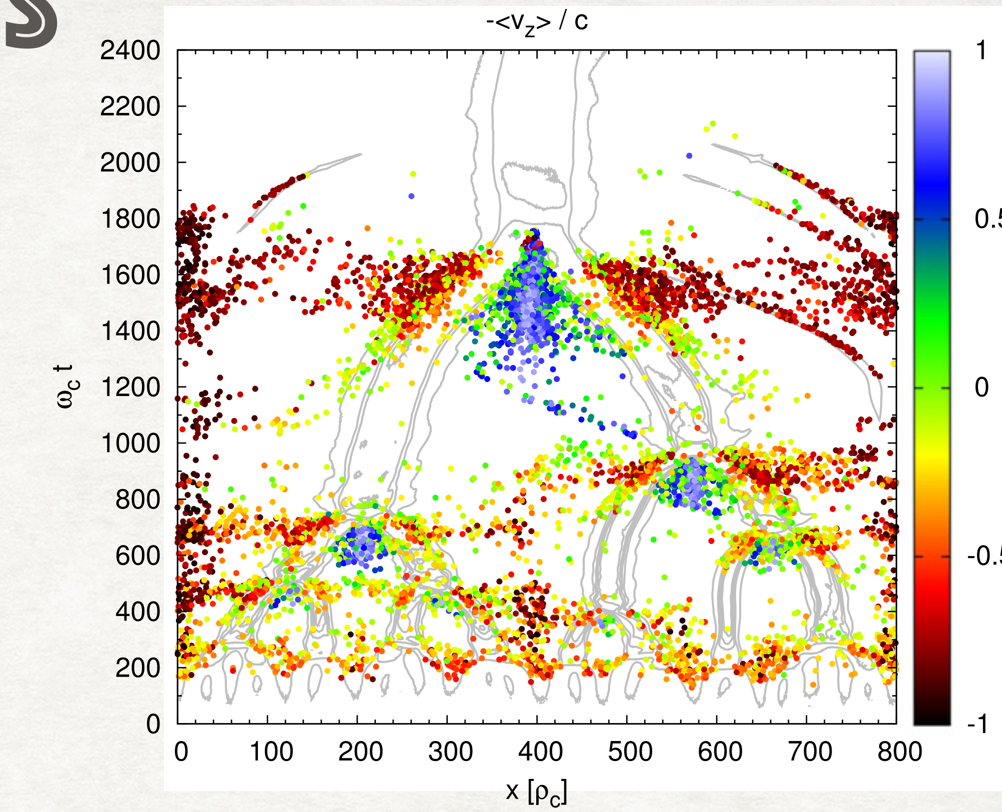

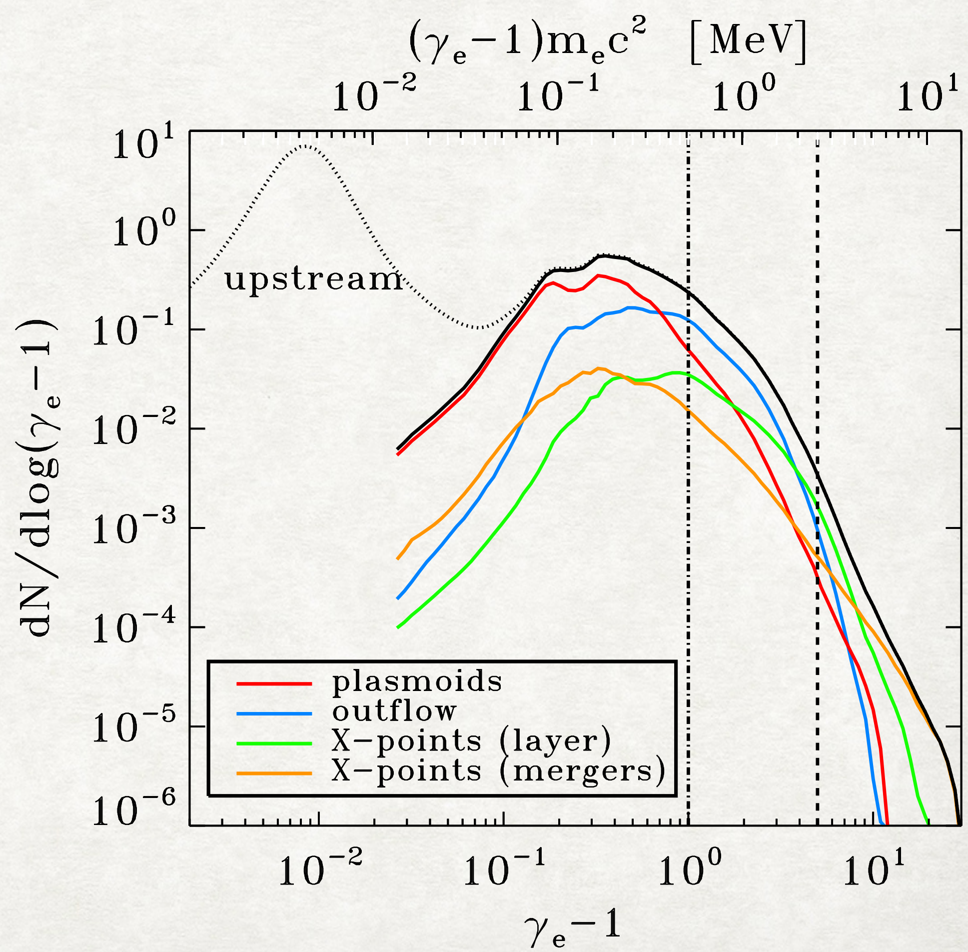

Sironi & Beloborodov (2020)

PLASMOID RECONNECTION WITH OPEN BOUNDARIES

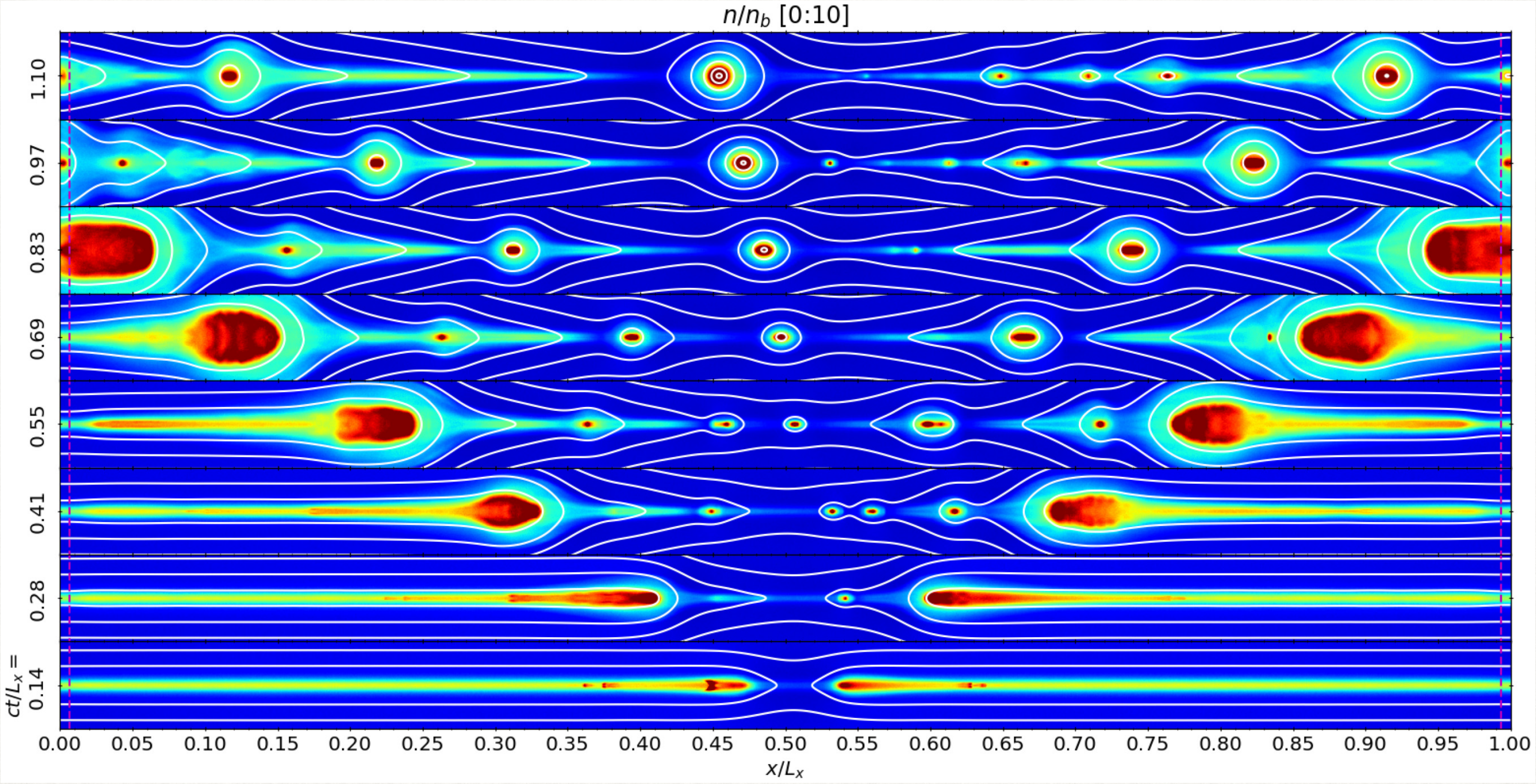

see also

J. Ortuño-Macías & KN (2020)

Daughton et al. (2006)

Sironi et al. (2016)

Particle-in-cell simulation of relativistic reconnection with open boundaries

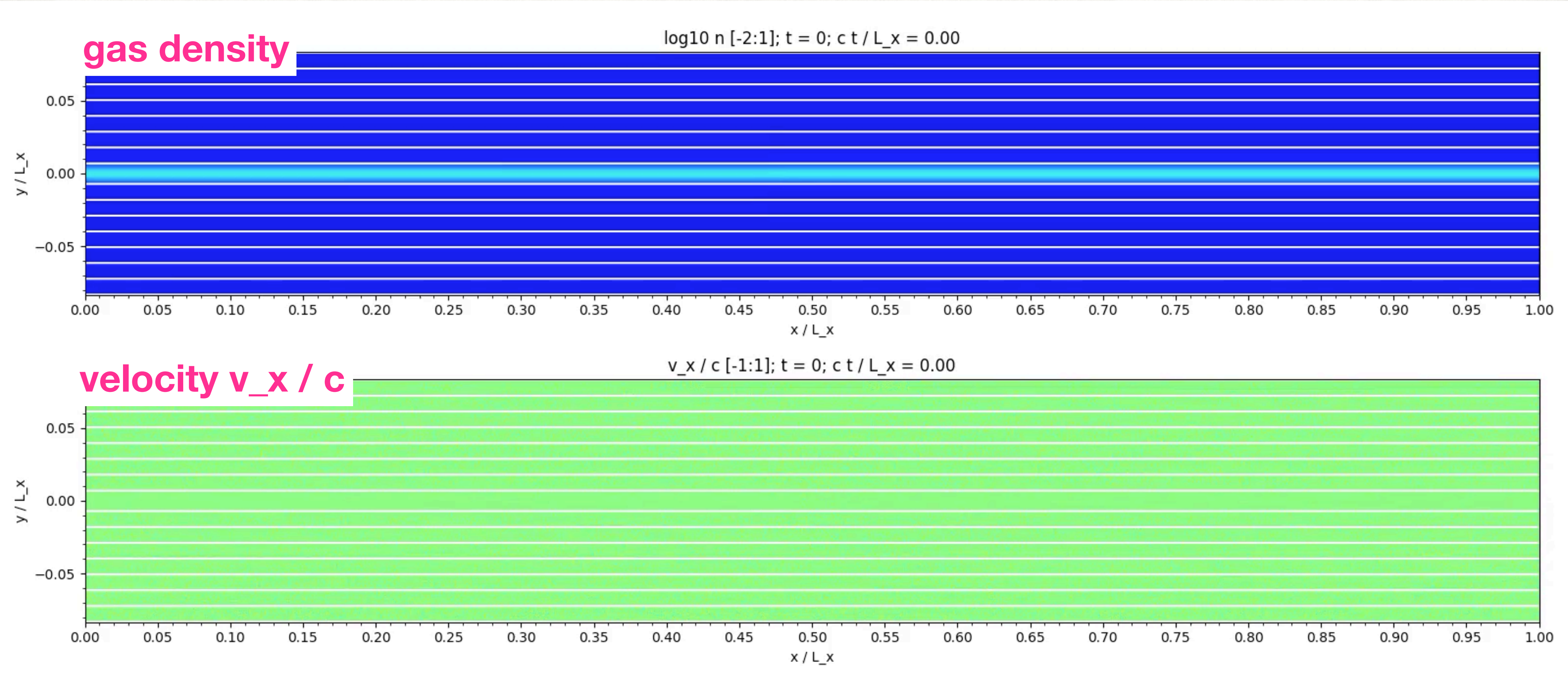

- left/right boundaries: freely outflowing particles, injection of inflowing particles, absorption of field perturbations
- fixed tall domain with $L_y = 4\ L_x$ for long steady-state simulations

J. Ortuño-Macías & KN (2020)

PARTICLE-IN-CELL SIMULATION OF RELATIVISTIC RECONNECTION WITH OPEN BOUNDARIES

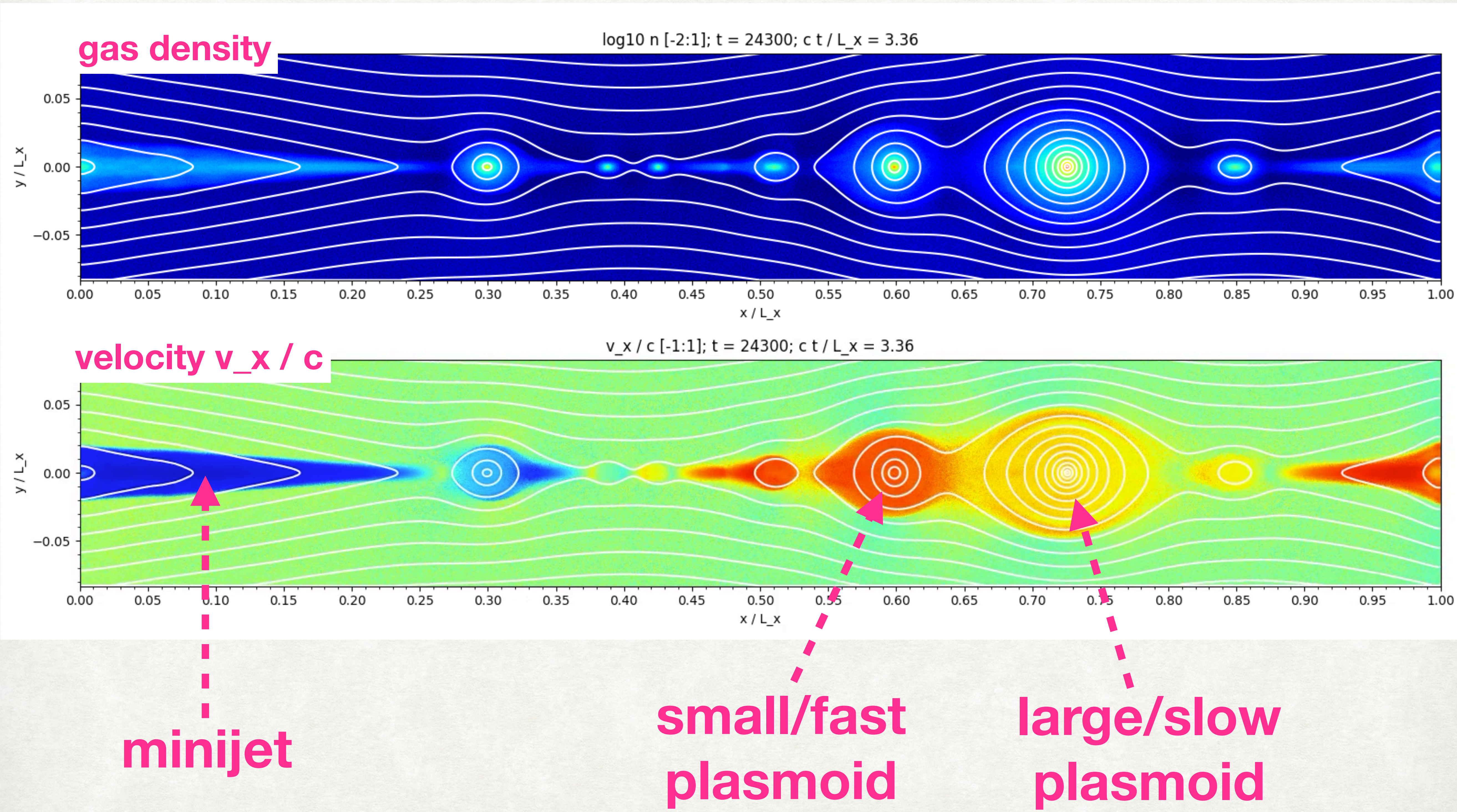

J. Ortuño-Macías & KN (2020)

RECONNECTION WITH OPEN BOUNDARIES: SPACETIME DIAGRAMS

magnetic field B_y | velocity v_x | gas density | mean particle energy in co-moving frame

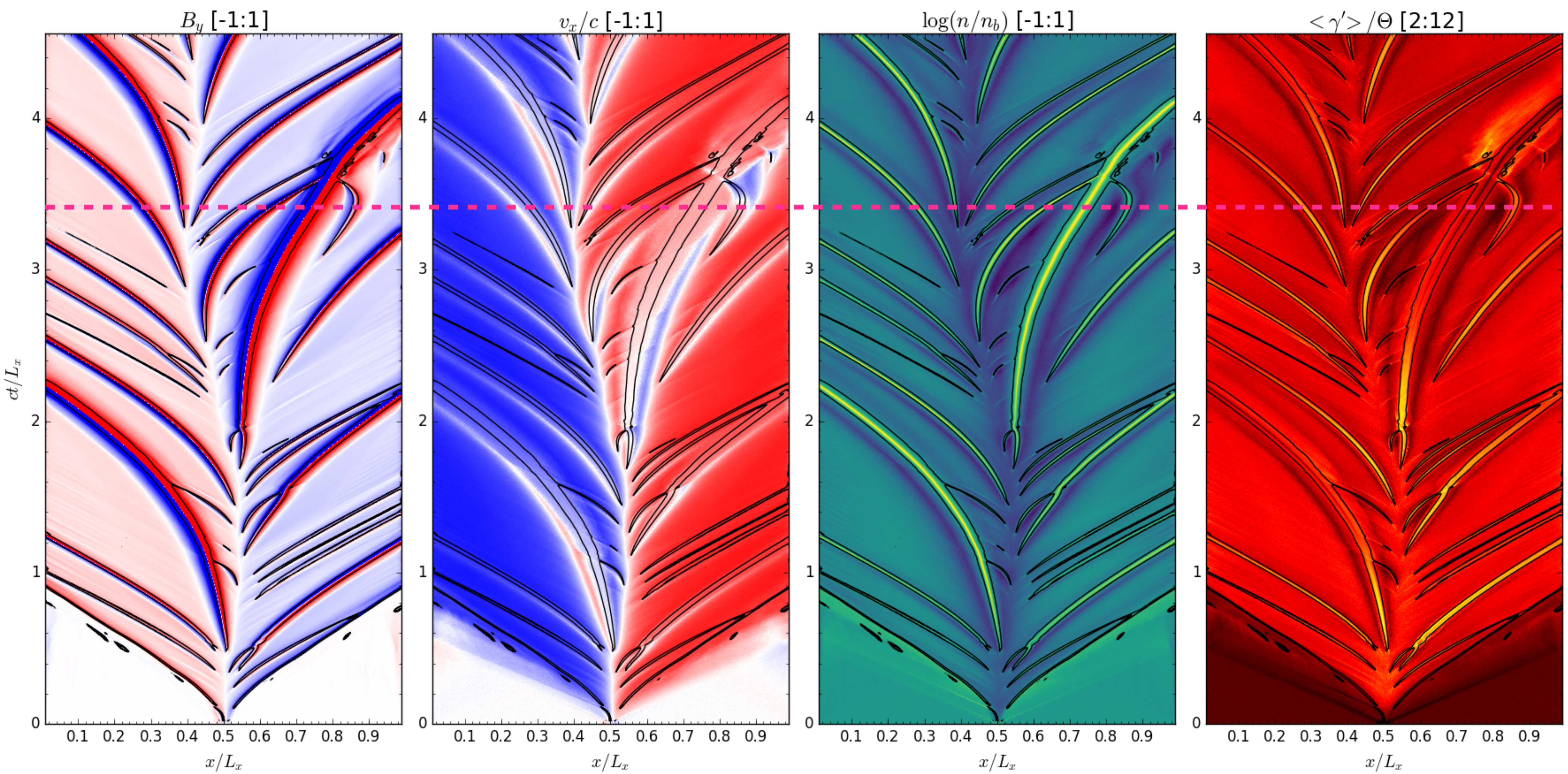

J. Ortuño-Macías & KN (2020)

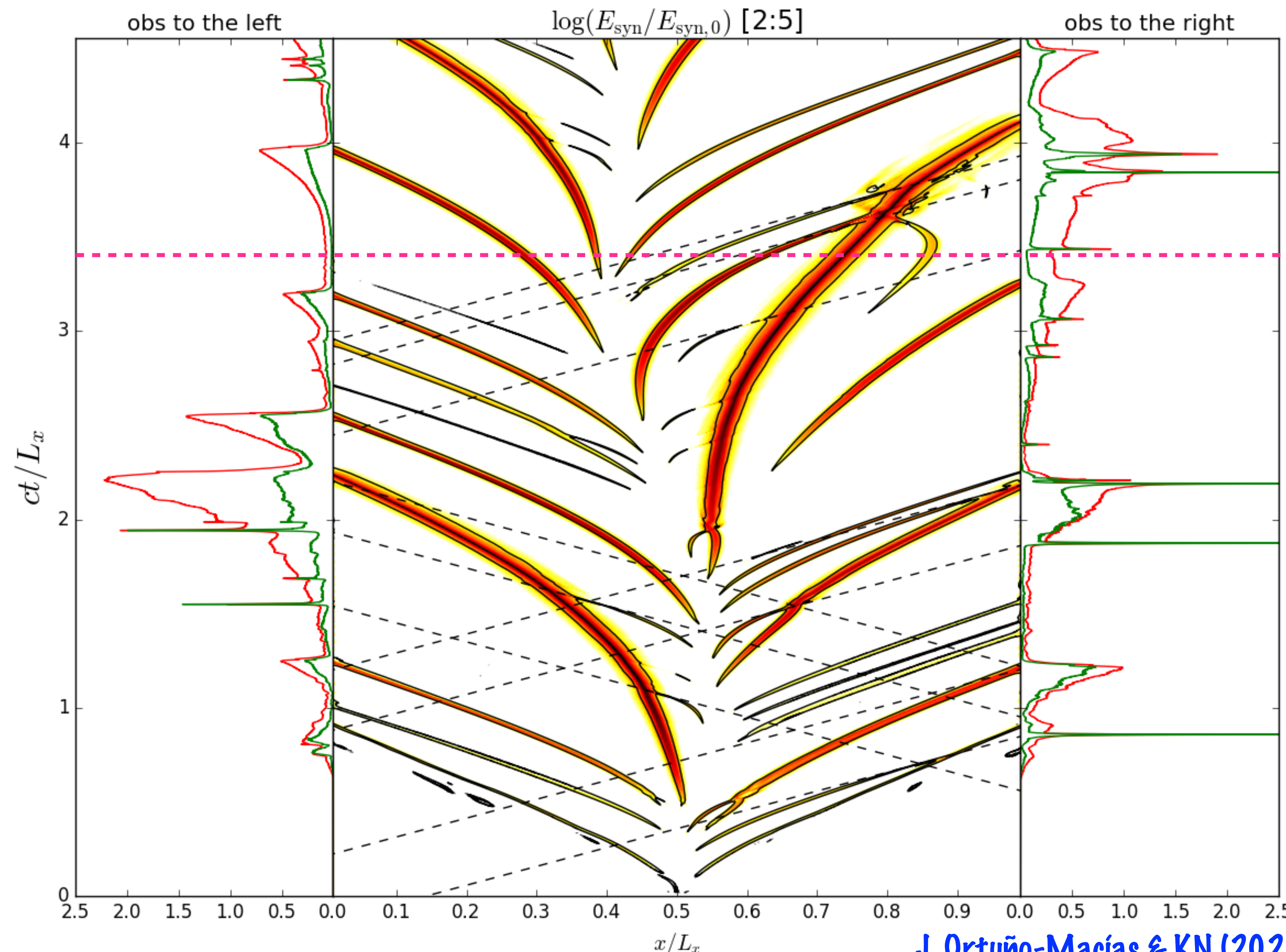

J. Ortuño-Macías & KN (2020)

Particle acceleration: plasmoids vs minijets

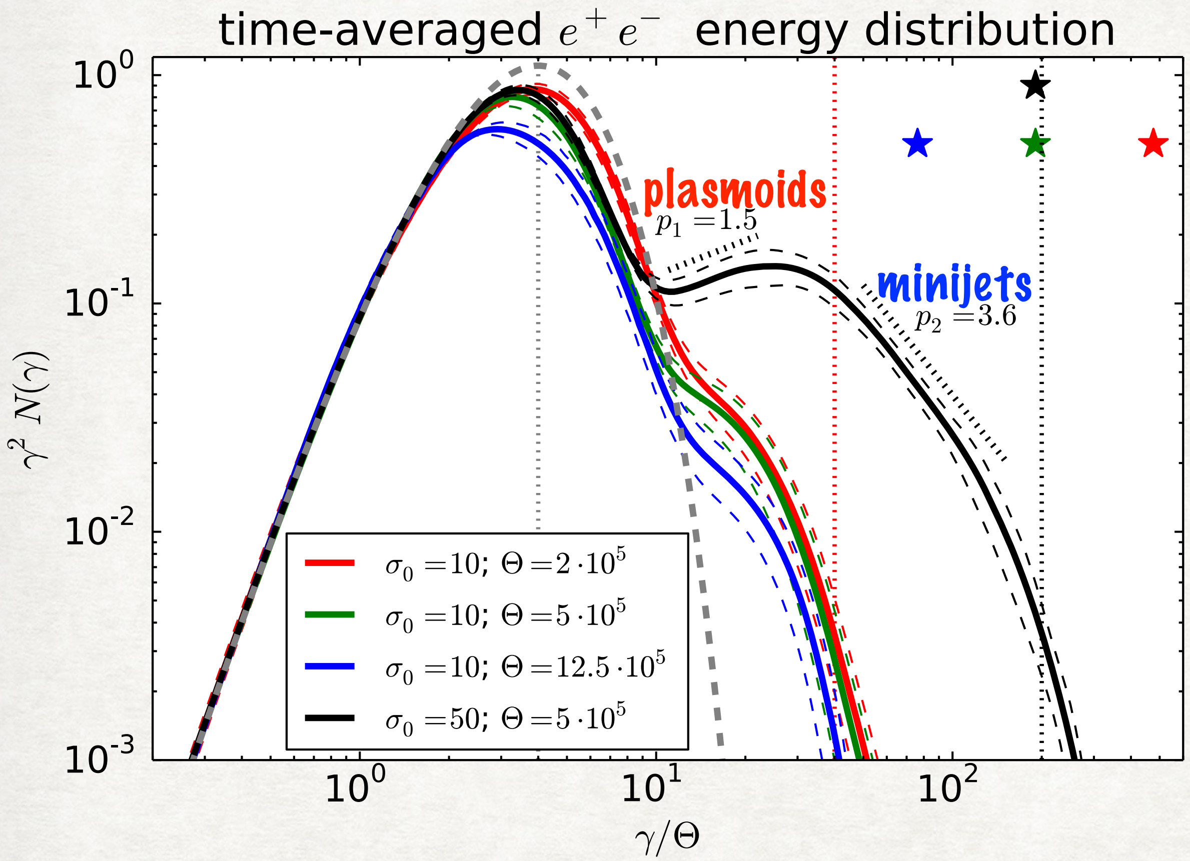

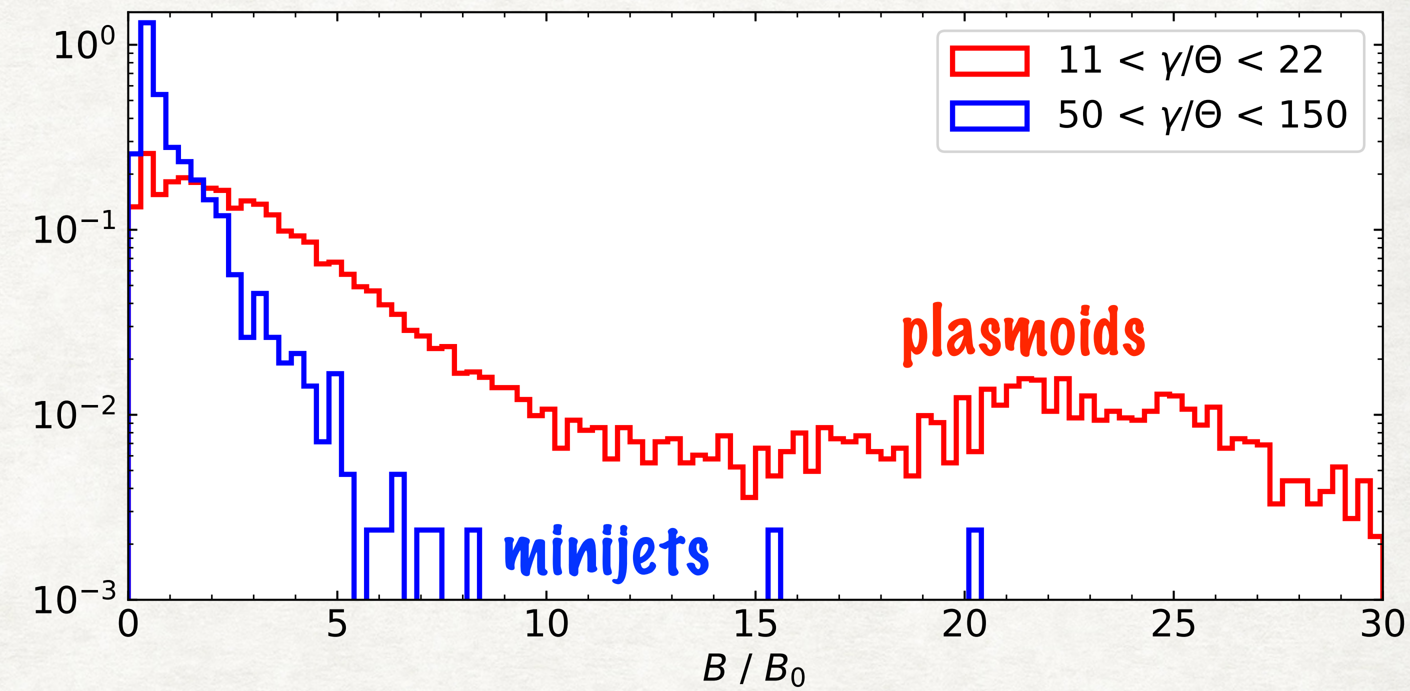

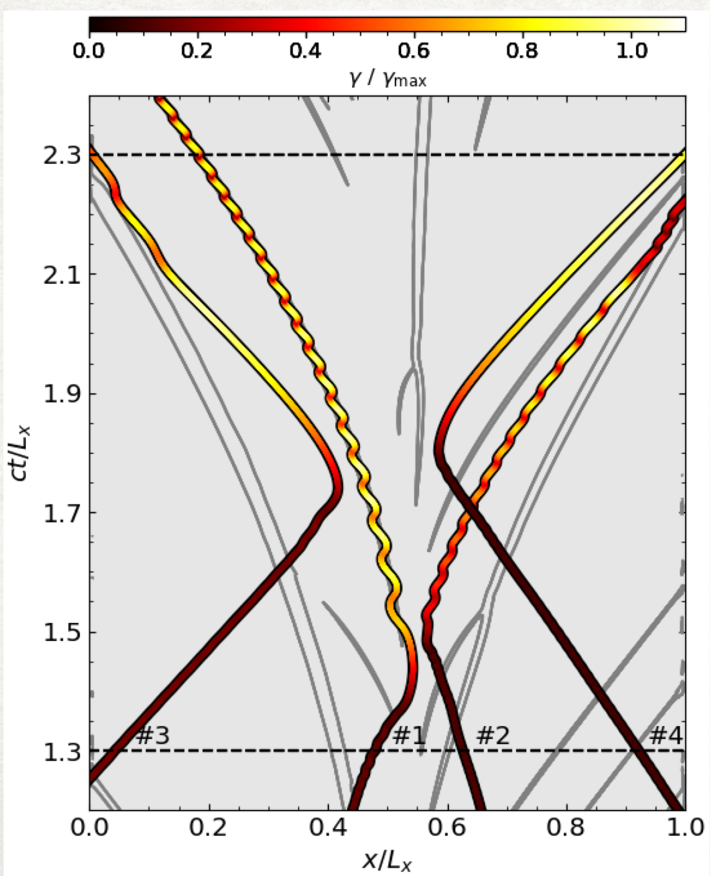

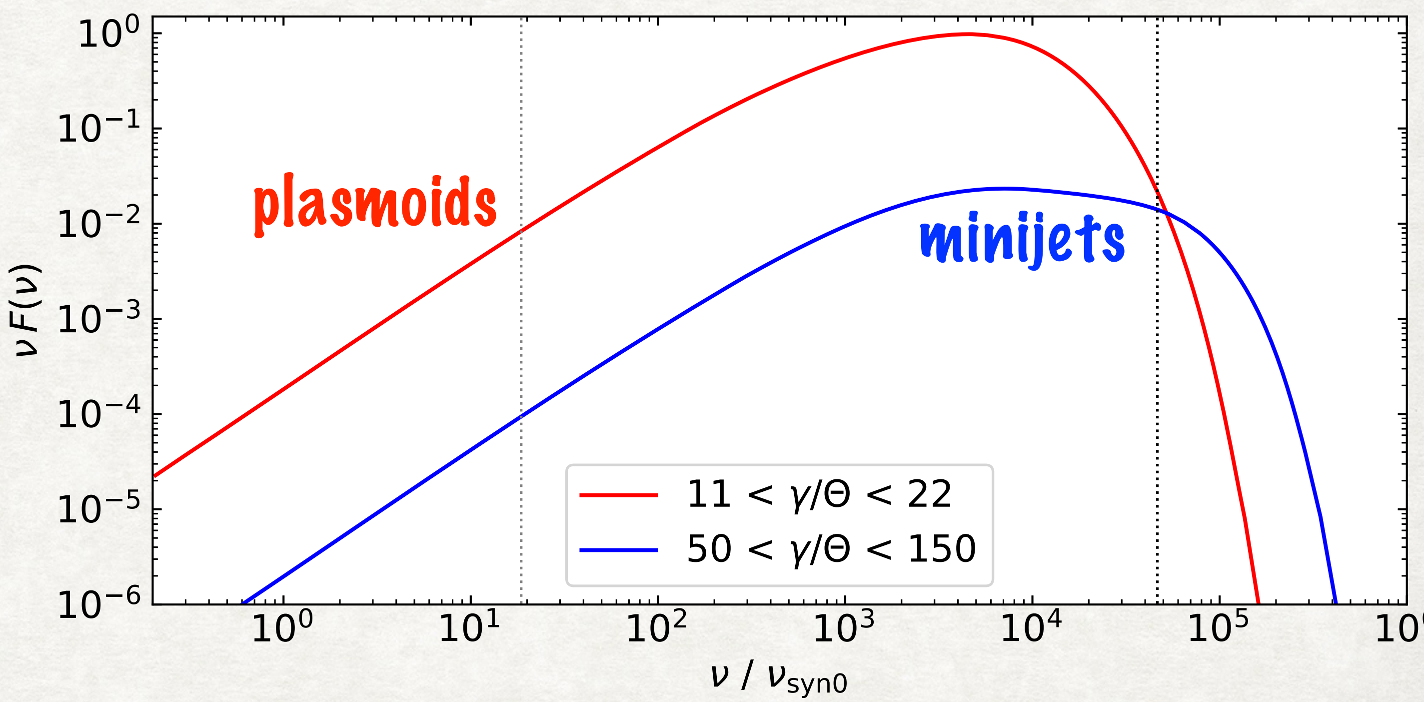

J. Ortuño-Macías & KN (2020)

Kinetic simulations of instabilities in cylindrical jets with toroidal magnetic fields

gas pressure balanced
(Z-pinch)

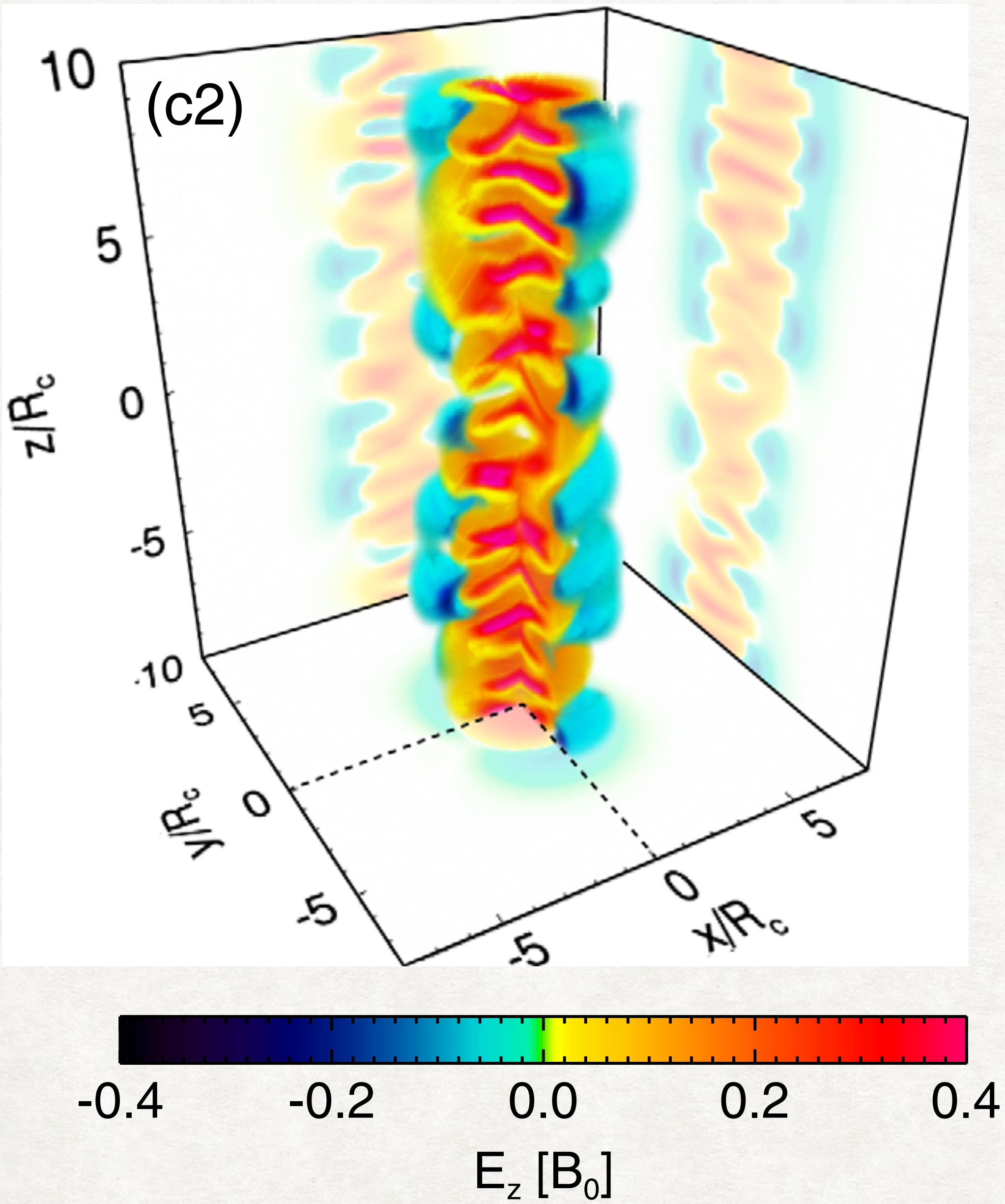

Alves, Zrake & Fiuza (2018)

axial magnetic field balanced
(force-free screw-pinch)

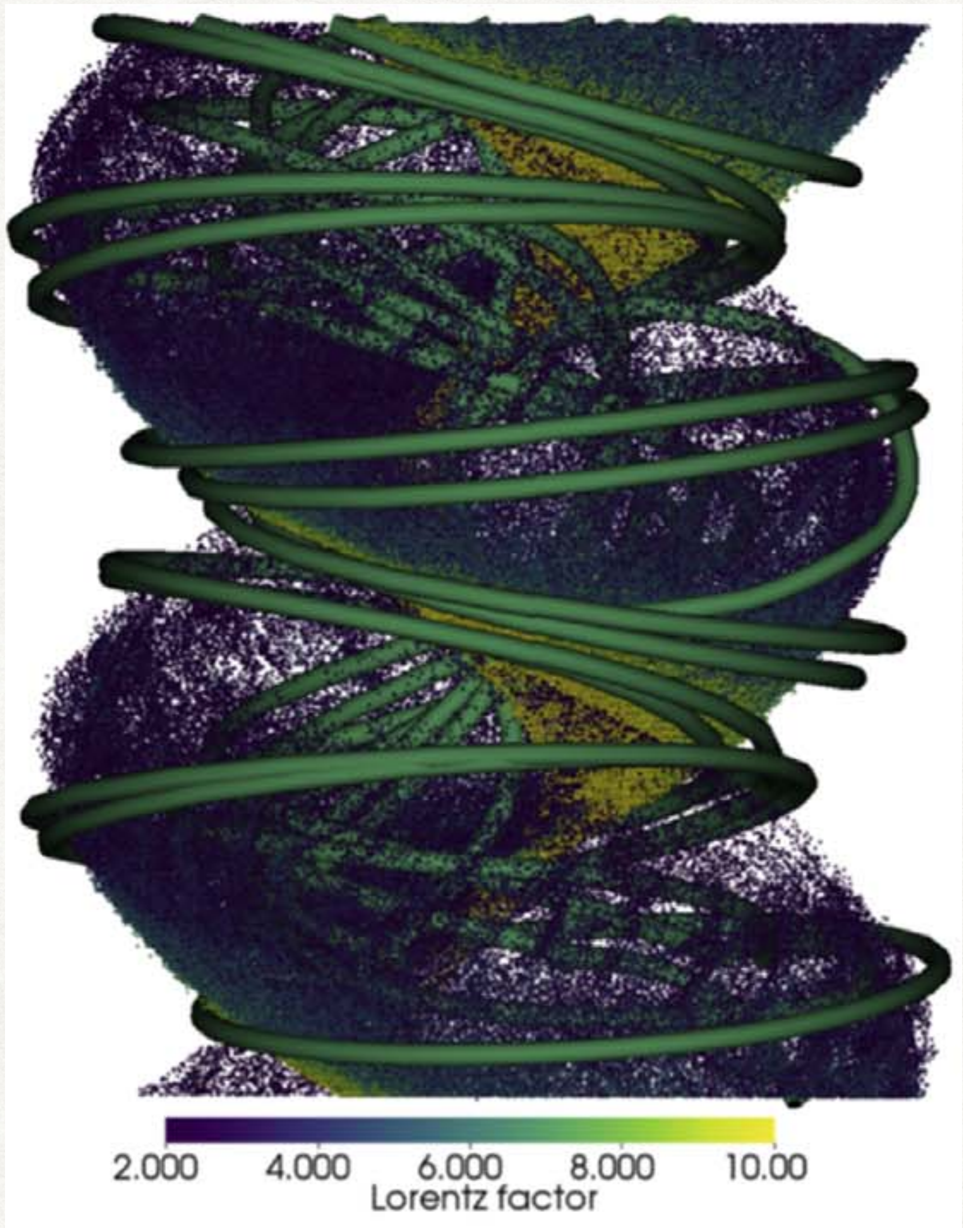

Davelaar, Philippov, Bromberg & Singh (2020)

efficient particle acceleration found in both cases; Hillas-type energy limit $E_{\rm lim} \sim eB_0R_{\rm core}$

KINETIC SIMULATIONS OF INSTABILITIES IN CYLINDRICAL JETS WITH TOROIDAL MAGNETIC FIELDS

3D, periodic boundaries, static equilibrium, pair plasma, moderately relativistic magnetization, highly relativistic temperature

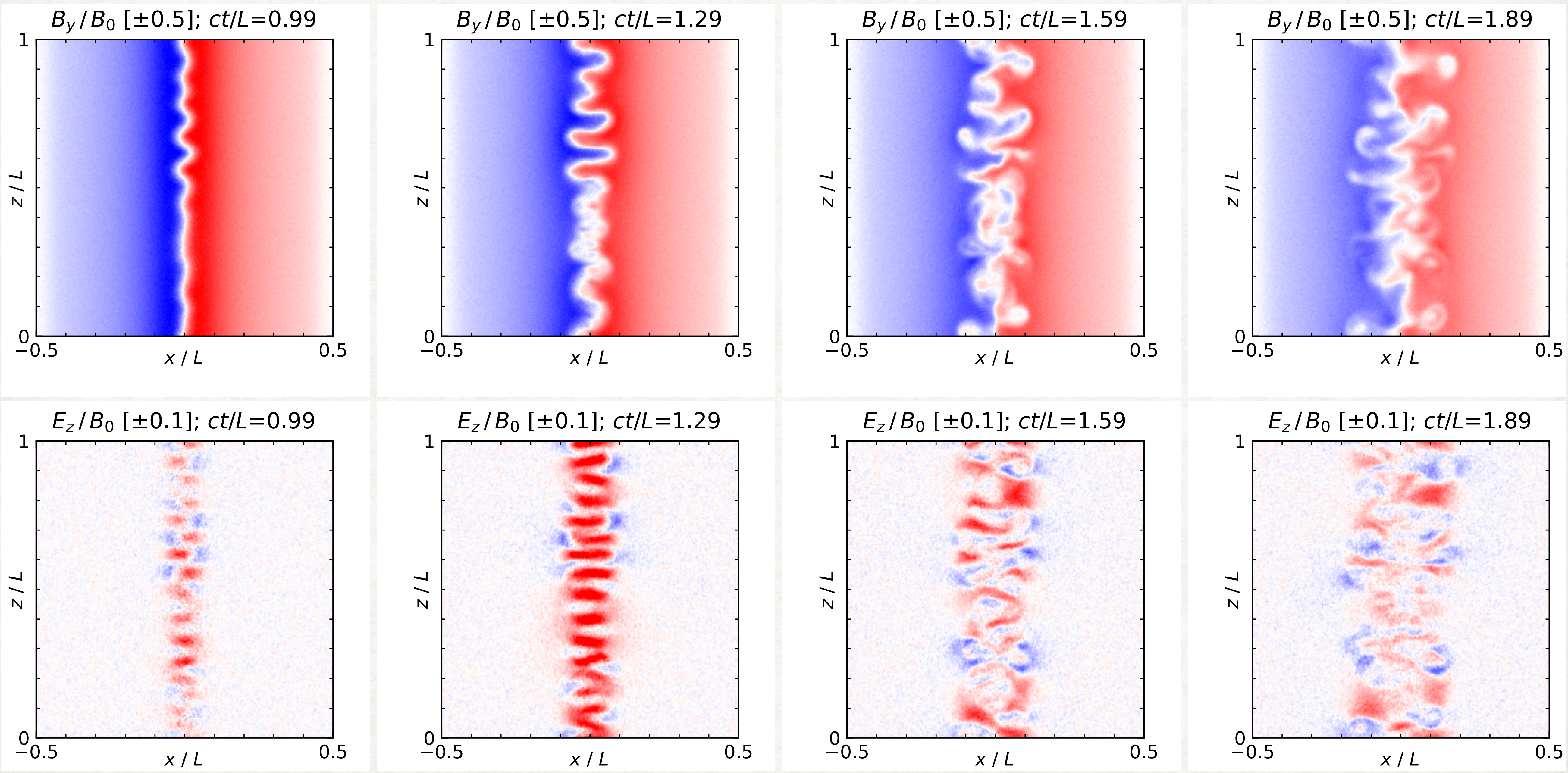

José Ortuño-Macías, KN, D. Uzdensky, M. Begelman, G. Werner, A. Chen, B. Mishra (2022)

TOROIDAL FIELD INDEX

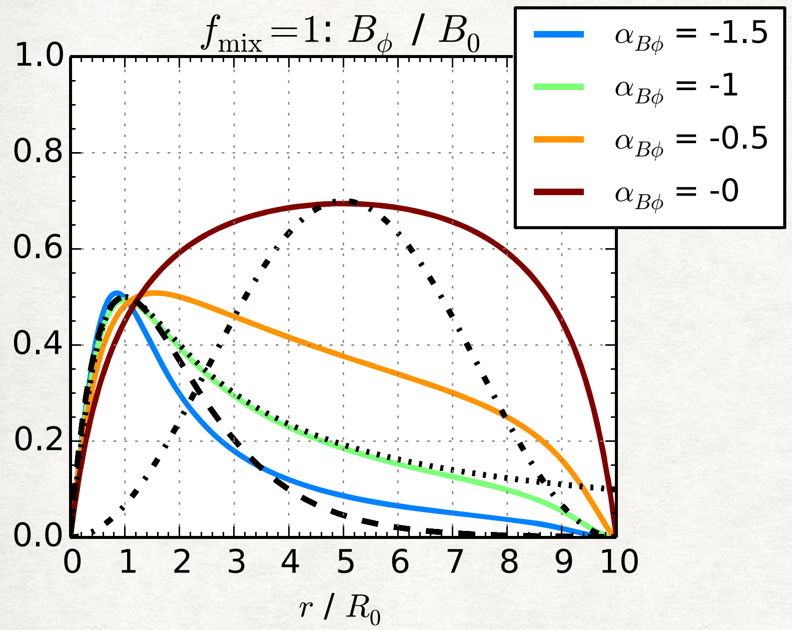

- Steep toroidal fields ($\alpha_{B\phi} \leq -1$) produce modes stalling at intermediate radii (a few R_0).
- Shallow toroidal fields ($\alpha_{B\phi} > -1$) produce modes propagating towards large radii.

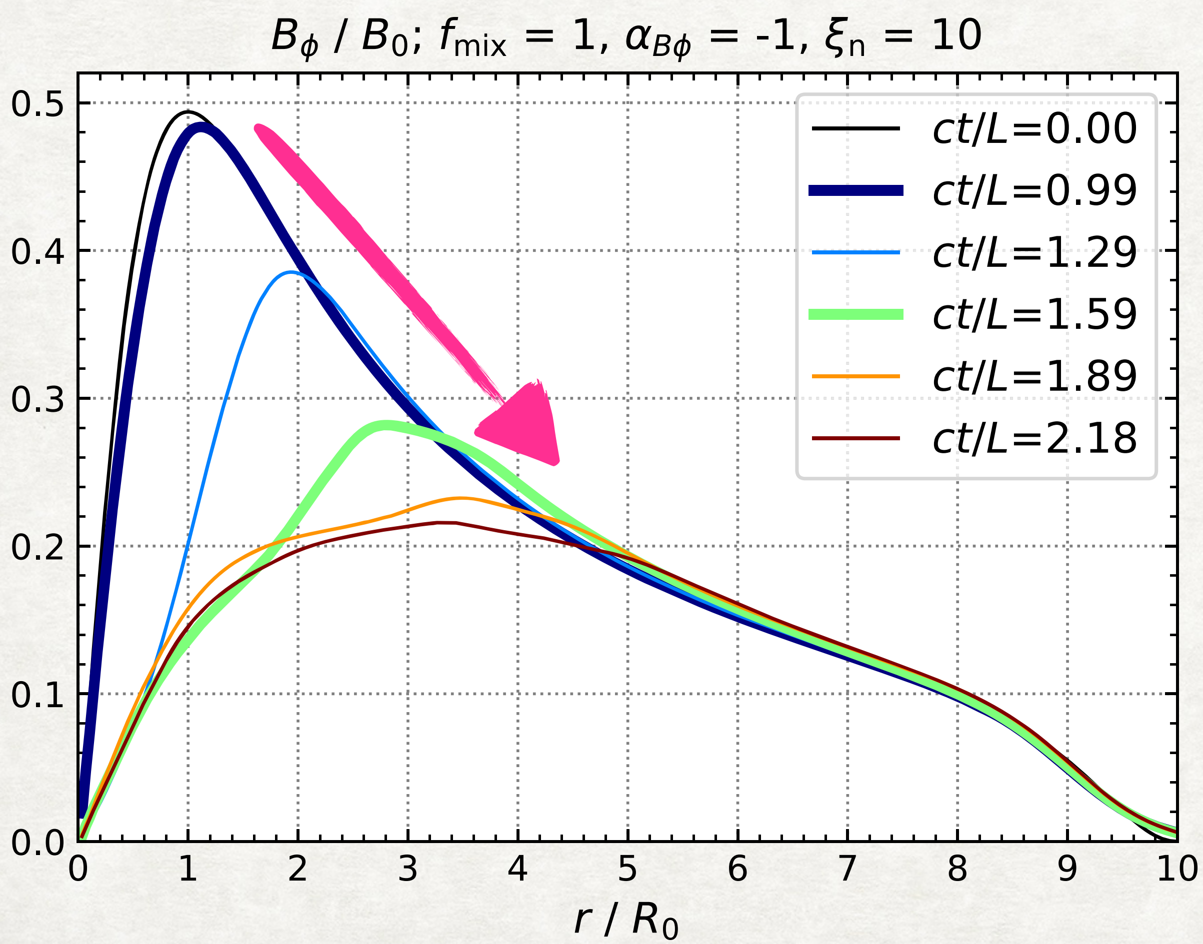

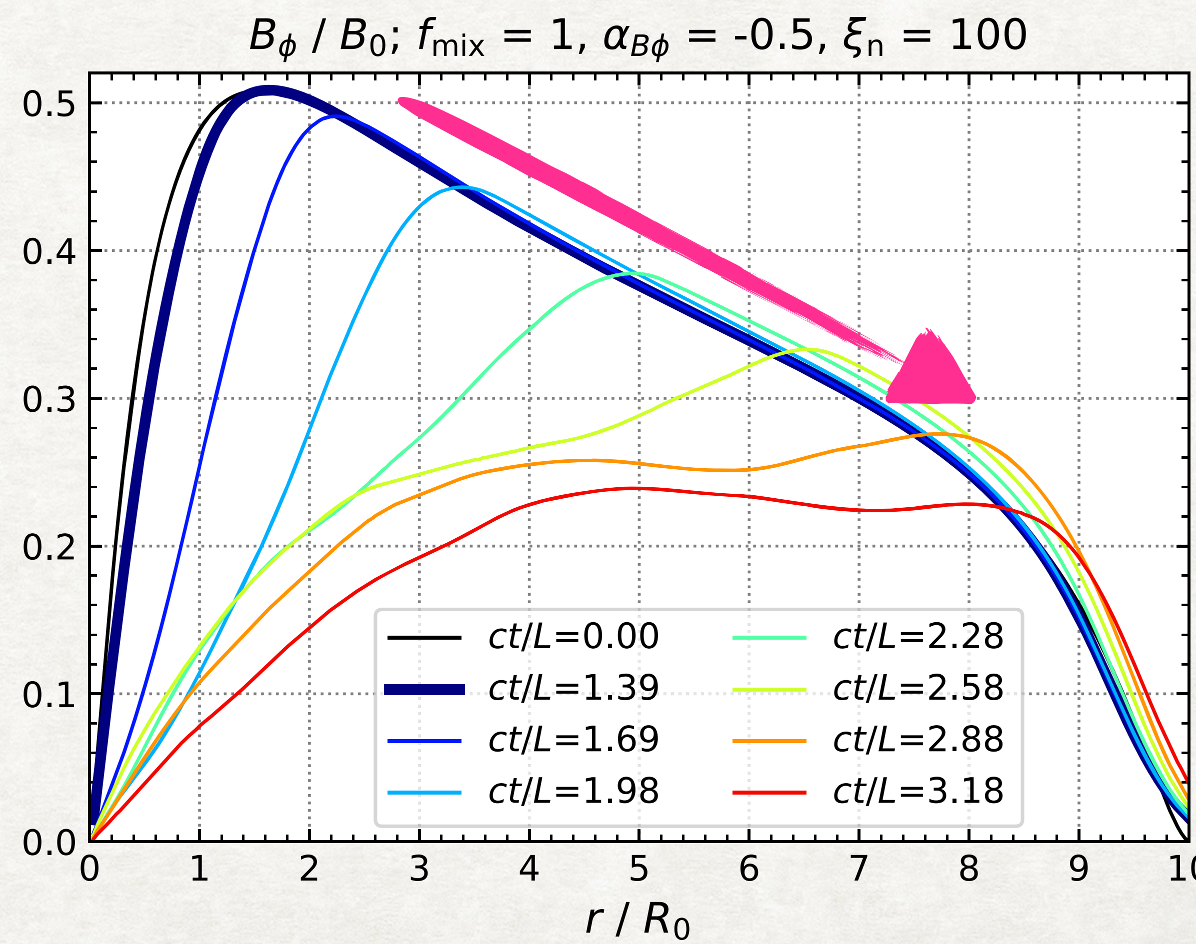

José Ortuño-Macías, KN, D. Uzdensky, M. Begelman, G. Werner, A. Chen, B. Mishra (2022)

Particle acceleration vs. magnetic dissipation

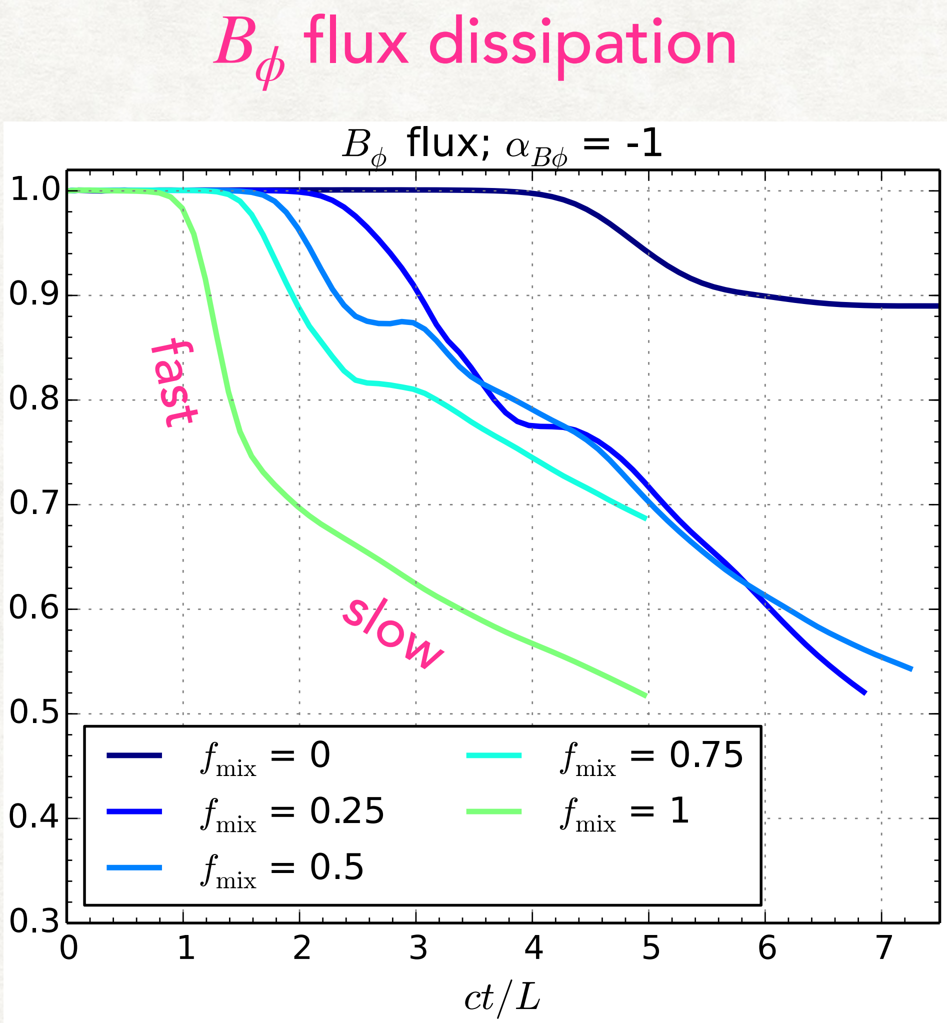

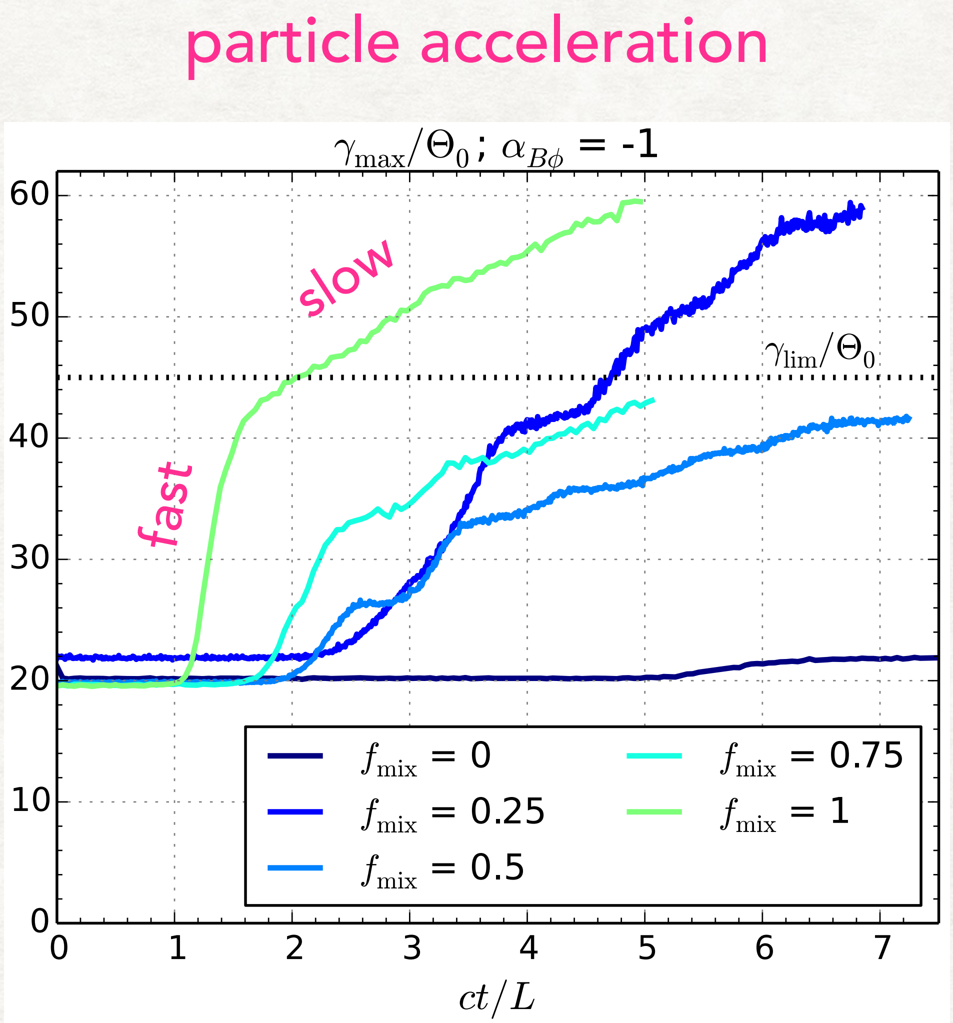

- rapid particle acceleration until the confinement limit $\gamma_{\rm lim} = eB_0R_0/mc^2$ coincides with the fast magnetic dissipation phase

José Ortuño-Macías, KN, D. Uzdensky, M. Begelman, G. Werner, A. Chen, B. Mishra (2022)

„Black hole flares"

temperature plasma beta mass density

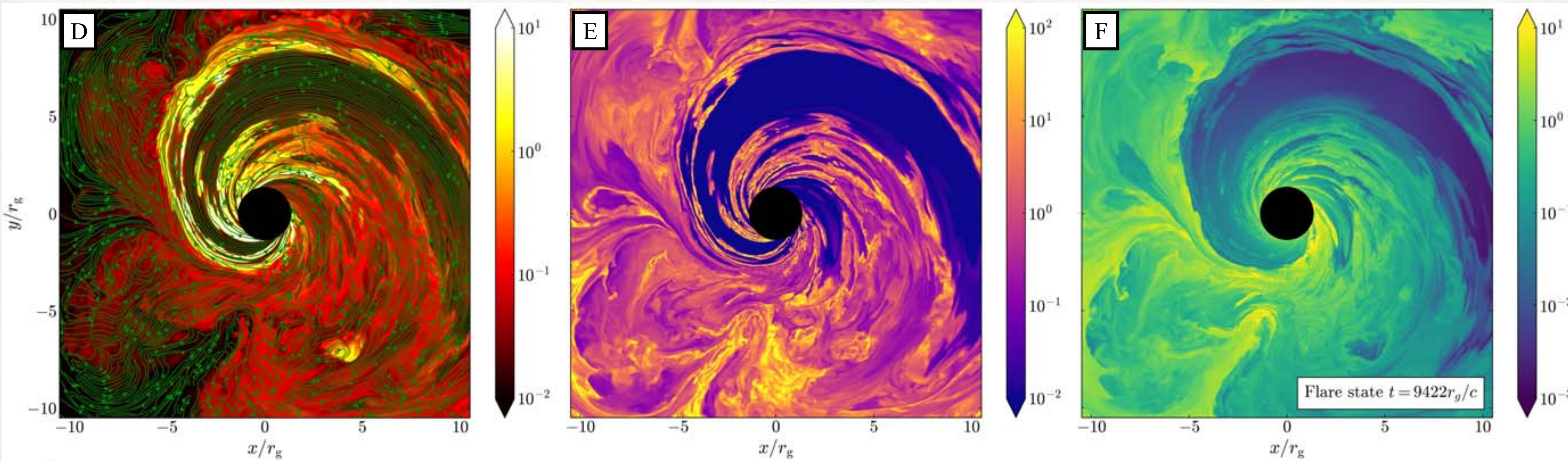

Ripperda et al. (2022)

- „Magnetically arrested disks" accumulate large magnetic fluxes at the BH horizon.
- Magnetic reconnection in the plunging region can eject part of the accretion flow, driving outflows, heating and particle acceleration, cancelling much of the BH magnetic flux (possibly a saturation mechanism).
- Potential explanation of gamma-ray flares from misaligned AGN like M87, IC 310, and orbital hotspots in Sgr A*.

Summary

knalew@camk.edu.pl

- Relativistic magnetic reconnection is a promising dissipation mechanism in relativistic magnetized jets.
- Rapid progress in understanding relativistic reconnection has been made in recent years, primarily due to kinetic numerical simulations.
- Relativistic reconnection has been proven to be a very efficient mechanism of particle acceleration, with the particle distribution index $p \sim 1\text{-}2$ in the limit of $\sigma \gg 1$.
- Reconnection results in fast localized outflows (minijets) and hierarchical chains of dense plasmoids.
- Radiation produced at reconnection sites is characterized by rapid variability time scales, potentially explaining even the most extreme gamma-ray flares observed in relativistic jets and pulsar winds.
- Reconnection requires locally reversed magnetic field lines, may be triggered by plasma instabilities. Possibly regulates magnetic fluxes (jet powers) at accreting black holes.
- Magnetization of relativistic jets may be highly inhomogeneous, up to $\sigma \sim 10^3$ locally to account for particle acceleration in blazars.

Thank You!